Aerosol and Air Quality Research, 19: 247–271, 2019

ISSN: 1680-8584 print / 2071-1409 online
doi: 10.4209/aaqr.2018.07.0275

Pollution Characterization, Source Identification, and Health Risks of Atmospheric-Particle-Bound Heavy Metals in PM_{10} and $PM_{2.5}$ at Multiple Sites in an Emerging Megacity in the Central Region of China

Nan Jiang*, Xiaohan Liu, Shanshan Wang, Xue Yu, Shasha Yin, Shiguang Duan, Shenbo Wang, Ruiqin Zhang, Shengli Li**

Key Laboratory of Environmental Chemistry and Low Carbon Technologies of Henan Province, Research Institute of Environmental Science, College of Chemistry and Molecular Engineering, Zhengzhou University, Zhengzhou 450001, China

ABSTRACT

A total of 588 daily PM filters were collected at five sites in Zhengzhou, and the mass concentrations and sources of the elements were analyzed. The health risks and source regions of the particles and toxic elements were also estimated. The results indicated severe $PM_{2.5}$ and PM_{10} pollution, especially at traffic sites. Additionally, the PM_{10}-bound As far exceeded the Chinese standards. Although the total elemental levels were relatively low at the rural site, they were high at the GY site. High levels of crustal elements were also observed at the SSQ and HKG sites. Seasonal-variation analysis revealed that the crustal elements, more abundant in the PM_{10}, occurred at high levels in spring; the combustion-source elements, more abundant in the $PM_{2.5}$, caused significant pollution in winter; and the elemental concentrations were low in summer. The coefficients of divergence for the $PM_{2.5}$ were slightly higher than those for the PM_{10}. Vehicles, industry, coal combustion, oil fuel, dust, and biomass burning were important sources of the PM-bound elements. Although the ZM site was characterized by low traffic and high contributions from biomass burning and dust emission, the HKG site featured a high proportion of emissions from traffic sources, and the SSQ site was also highly affected by vehicular pollution. Whereas elements in the $PM_{2.5}$ largely originated in combustion sources, those in the PM_{10} received greater contributions from dust sources. The levels of As and Ni posed intolerable carcinogenic risks (CR) and, along with that of Pb, also demonstrated significant non-CR risks. Children were more sensitive than adults to these risks, and the daily intake pathway demonstrated the highest CR and hazard index (HI) values. Obvious differences in the CR and HI values were detected between the various sites, suggesting the necessity of multiple-site studies for health risk assessment. Jiyuan, Jiaozuo, Xuchang, and Zhoukou; Pingdingshan and Nanyang; and Jiyuan, Jiaozuo, Xinxiang, Anyang, and Kaifeng were the main potential sources of $PM_{2.5}$, PM_{10}, and As, respectively.

***Keywords*:** Toxic elements; Coefficient of divergence; Enrichment factors; Principal component analysis; Carcinogenic risks; Potential source contribution function.

INTRODUCTION

Over the past three decades, the rapid economic development, urbanization, and industrialization in China have caused atmospheric pollution to become a common phenomenon in megacities, and the primary pollutant is particulate matter (PM) (Ji *et al.*, 2014). PM_{10} (aerodynamic diameter $\leq$ 10 μm) and $PM_{2.5}$ (aerodynamic diameter $\leq$ 2.5 μm) have been attracting considerable attention in related research fields because of their important impacts not only on global and regional climate changes (Bytnerowicz *et al.*, 2007), as well as reduced visibility (Moosmüller *et al.*, 2009), but also in human cardiovascular diseases and wheezing (Brunekreef and Forsberg, 2005; Pope and Dockery, 2006; Bell, 2012; Dunea *et al.*, 2016).

Toxic elements, such as As, Pb, Ni, Cd, Cu, Zn, and Cr, are important trace components in $PM_{2.5}$ and PM_{10} with considerably higher concentrations in urban areas than natural background levels due to anthropogenic activities (Wu *et al.*, 2007; Okuda *et al.*, 2008; Fang *et al.*, 2010; Charlesworth *et al.*, 2011). As a result, for urban residents, relatively high potential risks to human health are caused by these elements in atmospheric particulates. For example, the multi-element risk of $PM_{2.5}$ through inhalation exposure

* Corresponding author.
E-mail address: jiangn@zzu.edu.cn (N. Jiang); rqzhang@zzu.edu.cn (R. Zhang)

was beyond the acceptable level in the metropolitan zone in Mexico (Diaz and Dominguez, 2009); for $PM_{2.5}$, Cr poses carcinogenic risks (CR), and As, Mn, and Cd, through direct inhalation, cause significant noncarcinogenic risks in Chengdu, a megacity of Southwest China (Li *et al.*, 2016); adults and children in Zhengzhou were exposed to cancer risks of $PM_{2.5}$-bound As, Ni, and Pb in winter and summer, in which children were more sensitive (Jiang *et al.*, 2018b). Moreover, the residents were also exposed to toxic elements through dermal absorption and ingestion due to PM deposition during indoor and outdoor activities. Therefore, further studies on human health risks should be calculated through three exposure pathways, i.e., inhalation, dermal absorption, and ingestion (Hu *et al.*, 2012; Jiang *et al.*, 2018e).

Zhengzhou, the capital of Henan Province, an emerging megacity in the central region of China, had a population of 9.72 million by the end of 2016, with a high population density of 1,306 persons per square km (Bureau of Statistics of Henan Province, 2017). In 2016, the consumption of coal and coke in above designated size industrial enterprises i.e., all industrial enterprises with revenue from principal business above 20 million RMB, by industrial sector amounted to 30.84 and 0.12 Mt, respectively; as a major transport hub of China, the freight traffic of 220.38 Mt and passenger traffic of 163.61 million persons were completed by all the transport modes of transportation, i.e., railways, highways, and civil aviation (Bureau of Statistics of Zhengzhou, 2017). The surrounding area of Zhengzhou has the highest highway density nationwide, and the ratio of freight traffic and passenger traffic by highways accounted for 87.4% and 67.3% of the total quantity of transport (data in 2016), respectively. Meanwhile, the length and area of paved roads increased rapidly, especially in 2014–2016, with an annual average growth rate of 8.3% and 10.2%, respectively (Fig. S1 in Supplemental Materials). By the end of 2016, Zhengzhou demonstrated an annual gross domestic product of RMB 811.4 billion (the exchange rate of RMB 6.95 to USD 1), which is an 8.5% increase from the previous year (Bureau of Statistics of Zhengzhou, 2017), and with the extensive economic growth mode, $PM_{2.5}$ and PM_{10} pollution is serious in Zhengzhou (Ministry of Environmental Protection of the People's Republic of China, 2017; Jiang *et al.*, 2018d). However, a few studies focused on the chemical characteristics and sources of $PM_{2.5}$ at a single site in Zhengzhou (Yu *et al.*, 2016; Jiang *et al.*, 2017; Wang *et al.*, 2017; Jiang *et al.*, 2018c, 2019), with results only representing the surrounding region and hence, are not enough to explain the pollution level in Zhengzhou. There is only one study involving spatial-seasonal distribution and sources of $PM_{2.5}$-bound polycyclic aromatic hydrocarbons at multiple sampling sites in Zhengzhou (Li *et al.*, 2019). However, no systematical study at multiple sites with various characteristics (i.e., rural, traffic, and urban sites) focuses on atmospheric-particle-bound heavy metals.

In this study, five typical sites were selected for $PM_{2.5}$ and PM_{10} sampling in Zhengzhou for one year. The mass concentrations of PM and trace elements were determined, and the main sources of elements in $PM_{2.5}$ and PM_{10} were identified by enrichment factor (EF), Pearson's correlation analysis (CA), cluster analysis, and principal component analysis (PCA). In addition, health risks of local residents caused by toxic elements in the particle phase were estimated through the exposure pathways of inhalation, dermal absorption, and ingestion. The potential sources of $PM_{2.5}$, PM_{10}, and the toxic elements were also studied. The results of this study can provide the local government with important information for policy consideration of elements in PM prevention and control.

MATERIALS AND METHODS

Data and Sampling Site Information

The latitude of Zhengzhou ranges from 34°16′N to 34°58′N, and the longitude ranges from 112°42′E to 114°13′E. Fig. 1 shows the map of five sampling sites, including rural (ZM), traffic (HKG), and urban sites (GY, SSQ, and XM). The detailed information of the sites is shown in Table 1.

In this study, a total of 588 daily PM filters (285 samples for $PM_{2.5}$ and 303 samples for PM_{10}) in the ambient air for all 5 sites were collected using samplers (TH-150AII, Tianhong, China) with polypropylene filters (diameter: 90 mm; Tianjin Xinyao, China) at a flow rate of 100 L min^{-1} in each season from January 2016 to January 2017, and the sampling was conducted from 09:00 to 08:00 of the following day. All filters were conditioned in a clean room under a constant temperature of 20 ± 5°C and relative humidity of 50 ± 5% for 48 h of pre- and post-samples, and then weighed using a high-precision electronic balance (precision: 10 μg; XS 205, Mettler Toledo, Switzerland). Each filter was weighed at least twice, and the values were acceptable with the difference within 0.03 mg. Then the PM samples were stored in a freezer (–20°C) before elemental analysis.

Elemental Analysis

X-ray fluorescence (XRF) spectroscopy is a widespread method for elemental analysis with high stability (U.S. EPA, 1999; Mancilla and Mendoza, 2012; Hadley, 2017). A total of 21 elements in $PM_{2.5}$ and PM_{10} were analyzed using an S8 TIGER wavelength dispersive XRF spectrometer (Bruker, Germany). The method detection limits range from 0.002 μg m^{-3} (Mg) to 0.021 μg m^{-3} (Fe). Field blank filters were analyzed to measure blank concentrations. More details are described by Wang *et al.* (2018).

Coefficient of Divergence

The coefficient of divergence (CD) was calculated to compare and evaluate the total deviations of elements in PM between different sampling sites, which is defined by the following formula (Wongphatarakul *et al.*, 1998; Feng *et al.*, 2007):

$$CD_{jk} = \sqrt{\frac{1}{p}\sum_{i=1}^{p}\left(\frac{X_{ij} - X_{ik}}{X_{ij} + X_{ik}}\right)^2} \quad (1)$$

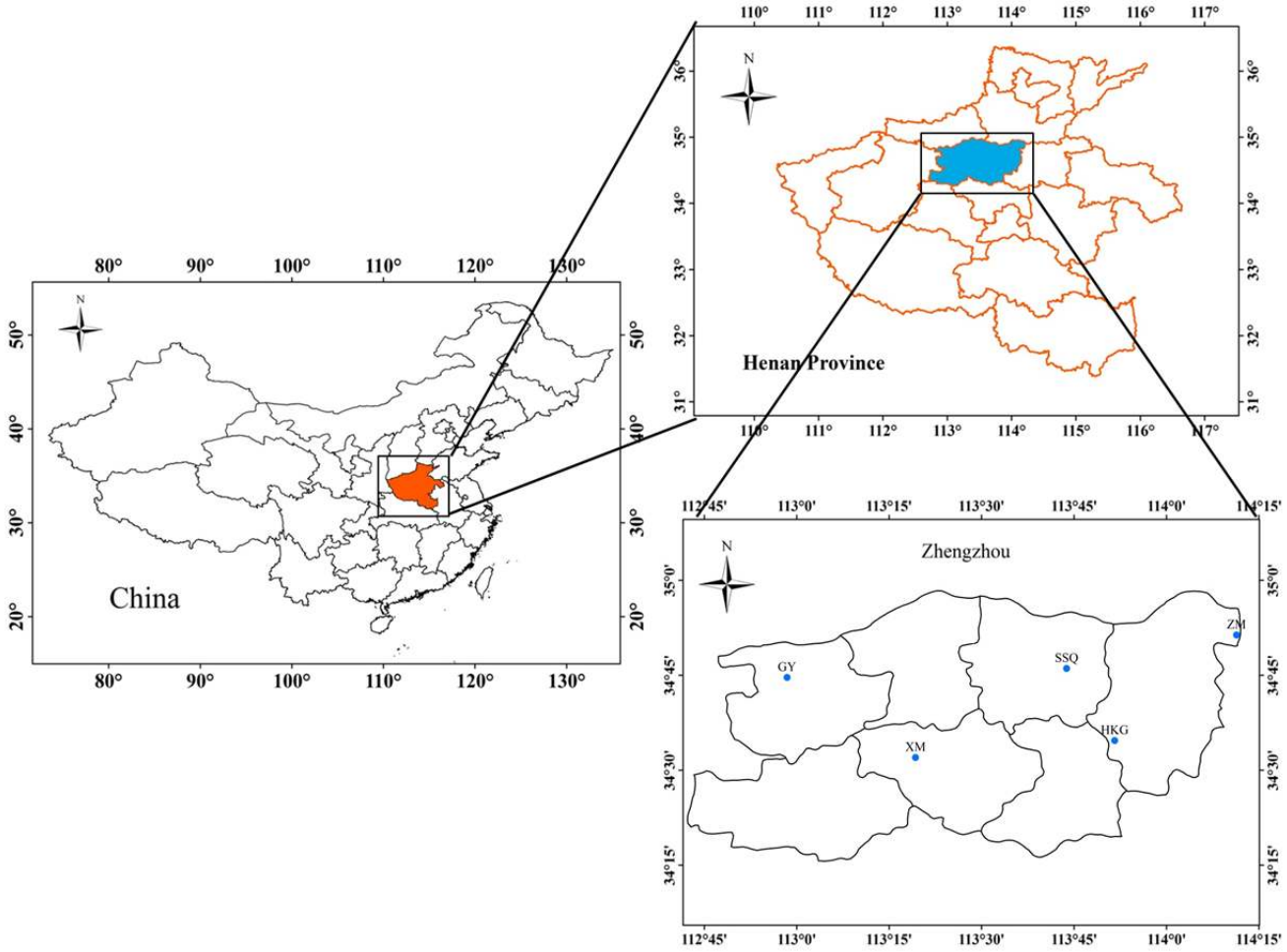

Fig. 1. Location of the sampling sites in Zhengzhou, China.

Table 1. Description of the sampling sites.

Category	Code	Longitude	Latitude	Location name	Description
Rural site	ZM	114°11′2″E	34°51′44″N	Zhongmu	Background site
Traffic site	HKG	113°51′46″E	34°34′59″N	Hangkonggang	One of the eight air hubs nominated by the Civil Aviation Administration of China, with the throughput of Xinzheng International Airport in 2016 over 20 million people http://www.ha.xinhuanet.com/hotnews/20161219/3582661_c.html
Urban site	GY	112°59′2″E	34°44′58″N	monitoring station of Gongyi	150 m from two urban main roads (Jianshe road and Renmin road) in Gongyi, a satellite city with the largest aluminum foil processing base in China http://sfjd.miit.gov.cn/BaseInfoAction!showBase.action?baseId=166
	SSQ	113°44′2″E	34°46′24″N	Forty-seventh middle school, the national monitoring network	High traffic with light-duty vehicles at downtown area
	XM	113°19′42″E	34°32′18″N	Xinmi	Next to the main road (Xidajie) in Xinmi, a satellite city with flourishing energy-intensive industries

where j and k represent two sampling sites; x_{ij} represents the mean concentration of element i at site j; p is the total number of elements. When CD_{jk} approaches zero, the result suggests that the two sites are similar for the chemical species, whereas when CD_{jk} approaches one, the two sites significantly differ. According to a previous study (Contini *et al.*, 2012), CD lower than 0.2 is selected for representing a relatively similar chemical composition.

Source Identification

In order to qualitatively evaluate contributions of different sources, i.e., anthropogenic sources and crustal origins, EFs are calculated as follows (Mason, 1966; Chao and Wong, 2002):

$$F = \frac{\left(C/Al\right)_{PM}}{\left(C/Al\right)_{Crust}} \tag{2}$$

where C is the concentration of trace element. Al is selected as the reference element (Hsu *et al.*, 2016). $(C/Al)_{PM}$ and $(C/Al)_{Crust}$ are the ratios of trace elements to Al in each PM sample and the upper continental crust, respectively, and the data of average crustal abundances are shown in a study on the element background values of Chinese soil (Wei, 1990). EF > 10 indicates that the element was generated from an anthropogenic source (e.g., coal combustion and vehicle emission); when EF is approximately equal to one, crustal origin is indicated (Nolting *et al.*, 1999).

Pearson's CA and cluster analysis, two of the most popular methods, were chosen to detect linear relationship (Robin *et al.*, 2013) and source contribution without source profiles (Viana *et al.*, 2008) of trace elements in $PM_{2.5}$ and PM_{10} at multiple sites through IBM SPSS for Windows, Version 22.0. Moreover, according to the species from the same source with similar characteristics (Ny and Lee, 2011), PCA was conducted for source identification of elements in PM by SPSS 22.0.

Health Risk Assessment

Exposure Assessment

Inhalation, ingestion, and dermal absorption are the main pathways of airborne toxic element exposure for local residents, i.e., children (< 15 years) and adults, divided by different respiration and behaviors (Hu *et al.*, 2012). According to U.S. EPA (1989, 2004, 2009), exposure concentration (EC; μg m^{-3}), chemical daily intake [CDI; mg $(kg\ d)^{-1}$], and dermal absorption dose [DAD; mg $(kg\ d)^{-1}$] of toxic elements in PM were calculated as the following equations. All the relative parameters were obtained from the official website of U.S. EPA, unless otherwise specified.

$$EC_{inhale} = \frac{\left(C \times ET \times EF \times ED\right)}{AT_1} \tag{3}$$

$$CDI_{ingest} = \frac{C \times IngR}{BW} \times \frac{EF \times ED}{AT_2} \times CF \tag{4}$$

$$DAD_{dermal} = \frac{C \times SA \times AF \times ABS}{BW} \times \frac{EF \times ED}{AT_2} \times CF \tag{5}$$

where C is the upper bound of the 95% confidence limit of the toxic elements in PM, μg m^{-3} or mg kg^{-1}; ET is the exposure time, 6 h d^{-1}; EF is the exposure frequency, 350 d $year^{-1}$; ED is exposure duration, 24 and 6 years for adults and children, respectively; AT_1 is the average time, AT_1 (for carcinogens) = lifetime years × 365 d $year^{-1}$ × 24 h d^{-1}, AT_1 (for noncarcinogens) = ED year × 365 d $year^{-1}$ × 24 h d^{-1}; lifetime is 74 years, which is the life expectancy in Henan (National Health and Family Planning Commission of the People's Republic of China, 2013); $IngR$ is the ingestion rate, 100 and 200 mg d^{-1} for adults and children, respectively; BW is the body weight, 59 (Wang *et al.*, 2009; National Bureau of Statistical of China, 2015) and 15 kg for adults and children, respectively; AT_2 is the average time, AT_2 (for carcinogens) = 74 years × 365 d $year^{-1}$, AT_2 (for noncarcinogens) = ED year × 365 d $year^{-1}$; CF is the conversion factor, 10^{-6} kg mg^{-1}; SA is the surface area, 5700 and 2800 cm^2 for adults and children, respectively; AF is the adherence factor, 0.07 and 0.2 mg $(cm^2\ d)^{-1}$ for adults and children, respectively; and ABS is the absorption fraction, 0.001, 0.03, and 0.01 for Cd, As, and other toxic elements (Hu *et al.*, 2012; U.S. EPA, 2017), respectively.

Risk Assessment

CR and hazard quotient (HQ) of toxic elements in PM were calculated for carcinogenic and noncarcinogenic risk assessment, respectively. The relative formulas are as follows (U.S. EPA, 1989, 2004, 2009):

$$CR = IUR \times EC = CDI \times SF_O = DAD \times \frac{SF_O}{GIABS} \tag{6}$$

$$HQ = \frac{EC}{\left(RfC_i \times 1000\ \mu g\ mg^{-1}\right)} = \frac{CDI}{RfD_O} = \frac{DAD}{RfD_O \times GIABS} \tag{7}$$

$$HI = \sum HQ_i \tag{8}$$

where all the upper parameter values for different elements were chosen according to U.S. EPA (2017); IUR is the inhalation unit risk, $(\mu g\ m^{-3})^{-1}$; SF_O is the slope factor, $[mg\ (kg\ d)^{-1}]^{-1}$; $GIABS$ is the gastrointestinal absorption factor; RfC_i is the inhalation reference concentrations, mg m^{-3}; $RfDo$ is the oral reference dose, mg $(kg\ d)^{-1}$; and HI is the hazard index for the three exposure pathways.

Trajectory Calculation

The hybrid single-particle Lagrangian Integrated Trajectory (HYSPLIT) model is a useful tool for assessing potential sources of pollutants. In this study, the model was used to obtain 48-h backward trajectories of air masses with an altitude of 500 m arriving at the urban site SSQ (34°46′24″N, 113°44′2″E) in Zhengzhou and with four trajectories each

day (00:00, 06:00, 12:00, and 18:00). Then, the potential source contribution function (PSCF) model, based on the HYSPLIT results, was used to identify the potential source regions of $PM_{2.5}$, PM_{10}, and toxic elements. The study region is equally divided into $i \times j$ grid cells, and the PSCF value in the ij^{th} cell is calculated by m_{ij}/n_{ij} (Ashbaugh *et al.*, 1985; Jeong *et al.*, 2011). n_{ij} and m_{ij} are the number of trajectories whose endpoints fall in the ij^{th} cell and the concentrations higher than the pollution criterion, respectively. According to the previous studies (Hsu *et al.*, 2003; Liao *et al.*, 2017), 75, 150 μg m^{-3}, and the average concentration of As were chosen as the pollution criterion for $PM_{2.5}$, PM_{10}, and toxic elements, respectively. The details of these methods were described by Ashbaugh *et al.* (1985) and Hopke *et al.* (1995). Uncertainties exist due to the small values of n_{ij}. Thus, to reduce the uncertainties, an empirical weight function, W_{ij}, was defined in the following formula. Then, the PSCF results were multiplied by W_{ij} (Polissar *et al.*, 1999; Zhang *et al.*, 2013). The domain was approximately in the range of 25–40°N, 105–120°E, with the resolution of 0.3° × 0.3°.

$$W_{ij} = \begin{cases} 1.00 & 80 < n_{ij} \\ 0.72 & 20 < n_{ij} \le 80 \\ 0.42 & 10 < n_{ij} \le 20 \\ 0.05 & n_{ij} \le 10 \end{cases} \quad (9)$$

RESULTS AND DISCUSSION

PM Mass Concentrations

Box-and-whisker plots for the concentrations of $PM_{2.5}$ and PM_{10} in Zhengzhou are shown in Fig. 2. The daily PM concentrations varied substantially among the sampling sites, i.e., $PM_{2.5}$: from 18 μg m^{-3} (XM) to 666 μg m^{-3} (SSQ) and PM_{10}: from 32 μg m^{-3} (ZM) to 819 μg m^{-3} (HKG). The average $PM_{2.5}$ concentrations decreased in the order of SSQ (143 ± 115 μg m^{-3}) > HKG (131 ± 91 μg m^{-3}) ≈ GY (130 ± 96 μg m^{-3}) > XM (113 ± 85 μg m^{-3}) ≈ ZM (112 ± 112 μg m^{-3}), whereas the mean PM_{10} values showed the order of HKG (196 ± 172 μg m^{-3}) > GY (190 ± 130 μg m^{-3}) > SSQ (181 ± 109 μg m^{-3}) > ZM (171 ± 134 μg m^{-3}) > XM (162 ± 137 μg m^{-3}). Generally, among the sampling sites, the rural site, i.e., ZM, was relatively slightly polluted; the traffic site, i.e., HKG, and the urban site with high traffic load, i.e., SSQ, showed relatively high $PM_{2.5}$ levels. HKG displayed the highest PM_{10} pollution because of its suburb-surrounded location with relatively high wind speed and poor dust control measures.

According to the Chinese National Ambient Air Quality Standards (NAAQS; daily $PM_{2.5}$: 75 μg m^{-3}; daily PM_{10}: 150 μg m^{-3}), from 47% (ZM) to 79% (SSQ) and from 38% (ZM and XM) to 60% (SSQ) of the sampling days for $PM_{2.5}$ and PM_{10}, respectively, exceed the standard. Among the sampling sites, the annual mean values of $PM_{2.5}$ (112–143 μg m^{-3}) and PM_{10} (162–196 μg m^{-3}) were 2.2–3.1 and 1.3–1.8 times higher than the NAAQS (annual $PM_{2.5}$: 35 μg m^{-3}; annual PM_{10}: 70 μg m^{-3}). In addition, these values were also found to be higher than megacities in the Yangtze River Delta region, the Pearl River Delta region and the Beijing-Tianjin-Hebei region in China, i.e., Shanghai ($PM_{2.5}$: 103 and 62 μg m^{-3}; PM_{10}: 149 and 97 μg m^{-3}) (Wang *et al.*, 2013), Guangzhou ($PM_{2.5}$: 61 and 45 μg m^{-3}; PM_{10}: 93 and 75 μg m^{-3}) (Peng *et al.*, 2011), and Beijing ($PM_{2.5}$: 102 μg m^{-3}; PM_{10}: 149 μg m^{-3}) (Guo *et al.*, 2010), not to mention the levels in the US ($PM_{2.5}$: 2–15 μg m^{-3}; PM_{10}: 4–21 μg m^{-3}) (Eldred *et al.*, 1997) and Europe ($PM_{2.5}$: 11–30 μg m^{-3}; PM_{10}: 19–38 μg m^{-3}) (Amato *et al.*, 2016). All of these present more serious PM pollution in Zhengzhou.

From a seasonal perspective, the mean concentrations of PM among the sampling sites in Zhengzhou are exhibited in Table 2. Obvious seasonal variations were observed, with the highest average concentrations in winter ($PM_{2.5}$: 235 ± 126 μg m^{-3}; PM_{10}: 308 ± 162 μg m^{-3}) and the lowest average values in summer ($PM_{2.5}$: 48 ± 17 μg m^{-3}; PM_{10}: 62 ± 18 μg m^{-3}). The reasons for these variations of PM

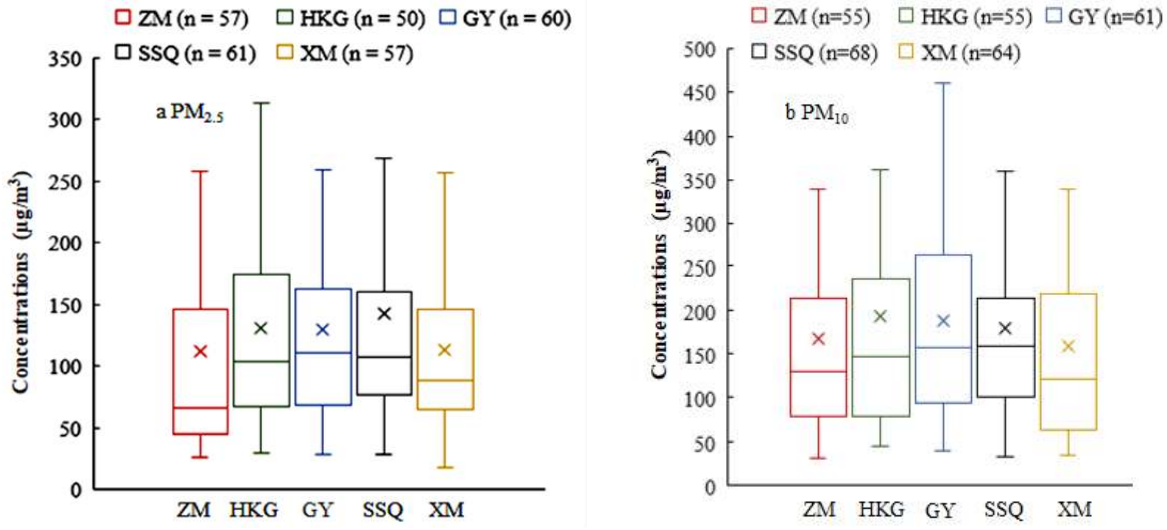

Fig. 2. Box-and-whisker plots for the $PM_{2.5}$ and PM_{10} concentrations among the sampling sites in Zhengzhou in 2016.

Table 2. Mean concentrations of PM among the sampling sites in Zhengzhou in 2016.

PM	Site	Spring		Summer		Autumn		Winter		Annual	
$PM_{2.5}$	ZM	84 ± 29	(n = 14)	48 ± 18	(n = 12)	50 ± 11	(n = 15)	244 ± 139	(n = 16)	112 ± 112	(n = 57)
	HKG	112 ± 44	(n = 13)	50 ± 11	(n = 10)	105 ± 34	(n = 13)	229 ± 109	(n = 14)	131 ± 91	(n = 50)
	GY	112 ± 28	(n = 16)	51 ± 15	(n = 14)	106 ± 33	(n = 15)	245 ± 124	(n = 15)	130 ± 96	(n = 60)
	SSQ	111 ± 36	(n = 15)	57 ± 15	(n = 13)	113 ± 27	(n = 15)	255 ± 156	(n = 18)	143 ± 115	(n = 61)
	XM	97 ± 22	(n = 14)	31 ± 13	(n = 12)	94 ± 51	(n = 14)	199 ± 97	(n = 17)	113 ± 85	(n = 57)
	Average	104 ± 34	(n = 72)	48 ± 17	(n = 61)	93 ± 40	(n = 72)	235 ± 126	(n = 80)	126 ± 101	(n = 285)
PM_{10}	ZM	122 ± 42	(n = 14)	57 ± 15	(n = 9)	114 ± 40	(n = 14)	309 ± 152	(n = 18)	171 ± 134	(n = 55)
	HKG	159 ± 48	(n = 13)	62 ± 17	(n = 15)	170 ± 70	(n = 12)	381 ± 200	(n = 15)	196 ± 172	(n = 55)
	GY	161 ± 34	(n = 16)	66 ± 19	(n = 14)	150 ± 56	(n = 13)	138 ± 141	(n = 18)	190 ± 130	(n = 61)
	SSQ	174 ± 52	(n = 16)	69 ± 21	(n = 13)	149 ± 38	(n = 14)	262 ± 127	(n = 25)	181 ± 109	(n = 68)
	XM	154 ± 47	(n = 14)	53 ± 11	(n = 14)	104 ± 77	(n = 15)	280 ± 169	(n = 21)	162 ± 137	(n = 64)
	Average	155 ± 47	(n = 73)	62 ± 18	(n = 65)	136 ± 62	(n = 68)	308 ± 162	(n = 97)	180 ± 136	(n = 303)

All concentration units are in μg m^{-3}.

include not only the different sources of emissions, but also the variant meteorological conditions in four seasons. For example, a great deal of coal is combusted for heating in the northern cities in China in winter. Moreover, frequent stagnant meteorological conditions occur in this season, causing high PM pollution. In summer, generally, the planetary boundary layer (PBL) development is enhanced by high temperature and higher PBL influences the vertical dispersion of the pollutants (Yang *et al.*, 2015).

Elemental Levels and Comparability among the Different Sites

Elemental Levels among the Different Sites

The mean concentrations of 21 elements in PM in Zhengzhou are summarized in Figs. 3, S2 and S3. In general, among the sampling sites, these concentrations of elements in $PM_{2.5}$ and PM_{10} vary substantially. Crustal elements, i.e., Ca (from 1653 ± 1229 ng m^{-3} to 4935 ± 6279 ng m^{-3} and from 4357 ± 2110 ng m^{-3} to 8949 ± 4670 ng m^{-3}, respectively), Si (from 1218 ± 949 ng m^{-3} to 2925 ± 3298 ng m^{-3} and from 3142 ± 1633 ng m^{-3} to 5138 ± 3420 ng m^{-3}, respectively), Fe (from 766 ± 502 ng m^{-3} to 2015 ± 2183 ng m^{-3} and from 1900 ± 972 ng m^{-3} to 3516 ± 2186 ng m^{-3}, respectively), K (from 1437 ± 1544 ng m^{-3} to 1728 ± 1577 ng m^{-3} and from 1712 ± 1143 ng m^{-3} to 2424 ± 1682 ng m^{-3}, respectively) and Al (from 523 ± 395 ng m^{-3} to 1408 ± 1240 ng m^{-3} and from 1378 ± 789 ng m^{-3} to 2326 ± 1210 ng m^{-3}, respectively) were the most abundant. According to the previous studies (Han *et al.*, 2010; Li *et al.*, 2017), these crustal element concentrations were considerably higher than those in Beijing, Shenyang, and Anshan in North China; meanwhile, the ratio of ∑crustal elements/PM (i.e., proportion of the five total crustal elements in PM) was approximately in the range of 7–10% and 9–13% for $PM_{2.5}$ and PM_{10}, respectively, in Zhengzhou and also much higher than those in Beijing (3–4%), Shenyang and Anshan (both approximately 1%). The elements associated with combustion, i.e., S (from 3150 ± 2171 ng m^{-3} to 3965 ± 3205 ng m^{-3} and from 3502 ± 3365 ng m^{-3} to 5067 ± 4088 ng m^{-3}, respectively), and Cl (from 1051 ± 1268 ng m^{-3} to 2981 ± 2502 ng m^{-3} and from 1259 ± 1493 ng m^{-3} to 3160 ± 2681 ng m^{-3}, respectively) were also plentiful in PM. The concentrations of S associated with $PM_{2.5}$ in Zhengzhou were far beyond those in Beijing (from 1.1 ± 1.1 μg m^{-3} to 1.3 ± 1.4 μg m^{-3} in $PM_{2.5}$) (Li *et al.*, 2017), with the former ratio of $S/PM_{2.5}$ (approximately 3–4%) also higher than the latter (approximately 1–2%). These results suggested that dust and combustion sources played more important roles in elemental levels of PM in Zhengzhou. Na, Mg, Zn, Ti, Pb, Mn, and Ba were present in moderate quantities, and Cu (except at the GY site), Sb, As, Se, V, Cr, and Ni were sparse in PM, with average concentrations almost lower than 50 ng m^{-3} among the sites. Though the toxic elements accounted for only a small fraction of PM, they should also be paid enough attention for their adverse health effects, especially for As, with all mean concentrations in PM_{10} (from 16 ± 15 ng m^{-3} to 28 ± 28 ng m^{-3}) far exceeding the Chinese NAAQS (annual As: 6 ng m^{-3}) among the sampling sites.

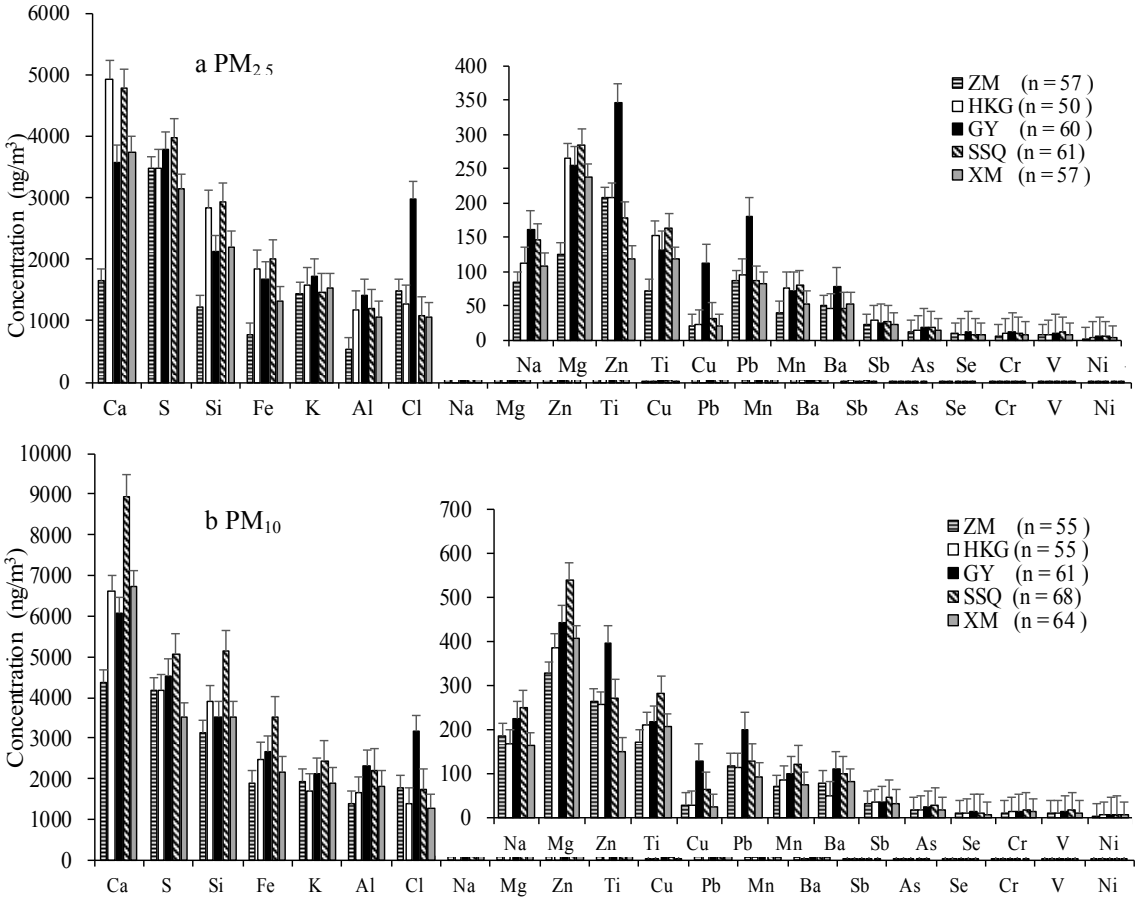

Fig. 3. Annual concentrations of elements in $PM_{2.5}$ and PM_{10} among the sampling sites in Zhengzhou in 2016.

For comparison, the total elemental concentrations varied obviously among different sites and decreased in the order: GY (18.70 μg m^{-3}) > SSQ (18.52 μg m^{-3}) > HKG (18.16 μg m^{-3}) > XM (14.91 μg m^{-3}) > ZM (11.28 μg m^{-3}) and SSQ (30.92 μg m^{-3}) > GY (26.34 μg m^{-3}) > HKG (23.33 μg m^{-3}) > XM (22.21 μg m^{-3}) > ZM (20.00 μg m^{-3}) in $PM_{2.5}$ and PM_{10}, respectively. Generally, the total elemental levels at the ZM site, defined as the rural site, are relatively low; in contrast to the variation tendency of PM, the total elemental concentrations at the GY site were high, especially Cl, Zn, Pb, and Cu, suggesting the important effects from combustion and vehicular sources (Zhang *et al.*, 2009; Bhangare *et al.*, 2011; Bozlaker *et al.*, 2013; Bozlaker *et al.*, 2014). High levels of crustal elements were observed at the SSQ and HKG sites, suggesting dust as one of main sources of elements in PM. Seasonal variations of element concentration were evident in Zhengzhou. Overall, among the sites, crustal elements, i.e., Ca, Si, Fe, K, and Al, demonstrated high levels in spring while elements from combustion presented relatively serious pollution in winter, and the elemental concentrations were low in summer. These phenomena are ascribed to the combined contribution of emissions and meteorological conditions. For example, lack of rain and high-speed winds are the typical spring climatic characteristics in North China (Zhang *et al.*, 2013) that result in increasing crustal element levels in PM. By comparing the elements with different diameters, crustal elements were found to be more abundant in PM_{10}, with the sum concentration of Ca, Si, Fe, K, and Al accounting for 63–73% of the total elements among the five sites, which were higher than those in $PM_{2.5}$ (50–68%). However, elements from combustion, i.e., S, Cl, Pb, As, and Se were more gathered in $PM_{2.5}$, with an average ratio (element in $PM_{2.5}$/element in PM_{10}) from 77% (As) to 87% (Se).

Comparability among the Different Sites

The CD values of elements in $PM_{2.5}$ and PM_{10} of the different sampling sites in this study are shown in Fig. 4. Among the sampling sites, the CD values obviously differed and ranged from 0.11 to 0.37 for $PM_{2.5}$ and 0.09 to 0.41 for PM_{10} during four seasons, which were almost higher than the annual CD values. On the whole, the CD values for $PM_{2.5}$ are slightly higher than those for PM_{10} from a seasonal perspective (except autumn), which may be due to the more complicated sources for fine particles than those for coarse particles. The CD values are not only related to discrepant spatial distribution of emission sources at the five sites but also attributed to different meteorological conditions in four seasons. Moreover, variant emission levels of elements have an effect on CD values. For example, a series of measures, including factories closed and production suspended, were conducted in the summer by the local government (Zhengzhou Municipal Environmental Protection Bureau, 2016). Measures were carried out to

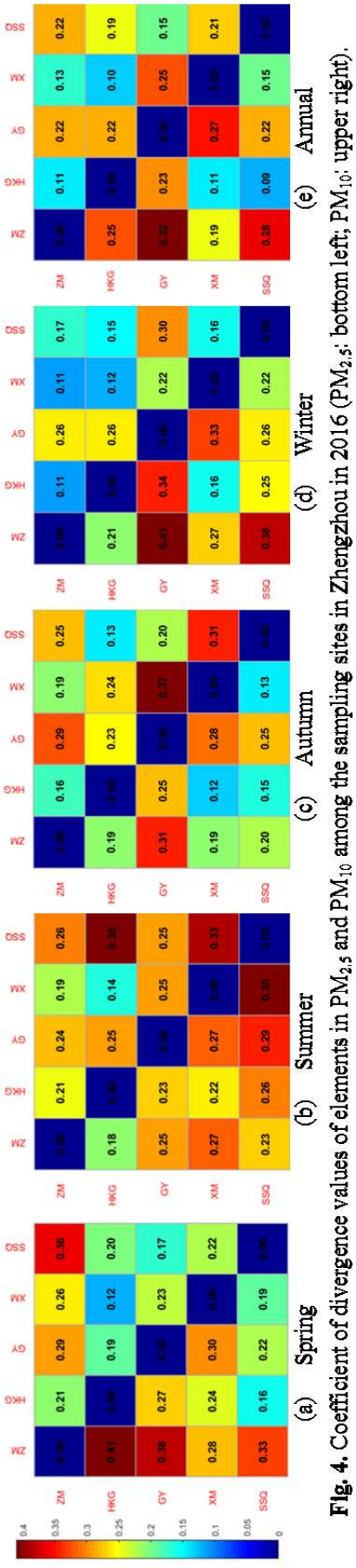

Fig. 4. Coefficient of divergence values of elements in $PM_{2.5}$ and PM_{10} among the sampling sites in Zhengzhou in 2016 ($PM_{2.5}$: bottom left; PM_{10}: upper right).

cooperate with the regional supervision centers, the organization set up by the Ministry of Environmental Protection of the People's Republic of China to monitor the implementation of environmental regulations.

Sources of Elements

The indicatory elements for various major sources, i.e., dust, coal combustion, traffic emission, industrial emission, oil fuel, and biomass burning, in previous studies are listed in Table 3. EFs, Pearson's CA, cluster analysis, and PCA were conducted to identify the main sources of elements in PM.

Enrichment Factors of Elements

The calculated EFs of elements in PM among the sampling sites in this work are displayed in Fig. 5. Na, Sb, Pb, Zn, Cu, and As were significantly enriched at all sites with high EFs ($PM_{2.5}$: 60–12,125; PM_{10}: 44–8,032), indicating anthropogenic sources. In the previous study, Na is mainly derived from coke-making, and cold-forming and hot-forming processes in iron and steel industries (Tsai *et al.*, 2007). Sb is emitted from industries, e.g., the steel or petrochemical industry (Querol *et al.*, 2006), and also from vehicular emissions (Charlesworth *et al.*, 2011). Smelting and coal combustion processes are considered to be the primary sources of Pb and As (Zhang *et al.*, 2009; Bhangare *et al.*, 2011). Zn and Cu are probably generated from abrasion of brake linings and tire tread wear (Bozlaker *et al.*, 2014). Therefore, industries, vehicles, and coal combustion are the main anthropogenic sources of elements in PM in Zhengzhou. The EFs of Si, Mg, and Ti are close to 1, indicating that crustal origin is also an important source of elements in aerosol (Nolting *et al.*, 1999). The EFs of other elements, i.e., K, Ca, Mn, Cr, Ba, V, Fe, and Ni, are between 1 and 10, suggesting the emission from anthropogenic and natural sources. For example, K is associated with dust (Jiang *et al.*, 2018a) and biomass burning sources (Silva *et al.*, 1999).

Pearson's Correlation and Cluster Analysis

Correlation of different elements is an important basis of source identification that can help to confirm and obtain interpretation of PCA results. Table 4 shows the Pearson's CA of elements in PM among the sampling sites in Zhengzhou. A significant correlation was observed among Na, Mg, Al, Si, Ca, Fe, and Mn in $PM_{2.5}$ and PM_{10} during the sampling period at the five sampling sites, suggesting that these elements were probably emitted from a common source. As and Se are highly correlated (0.51–0.88 for $PM_{2.5}$ and 0.53–0.88 for PM_{10}), indicating a similar source. High correlation coefficients were observed not only between Zn and Cu but also between Ni and V, demonstrating similar sources.

The cluster analysis results of elements in PM are shown in Figs. S4 and S5 in Supplemental Materials. Three clusters of elements in $PM_{2.5}$ and PM_{10} at the sampling sites, except for $PM_{2.5}$ at HKG and XM sites (four clusters), were chosen. Generally, Cluster 1 is characterized by Ni, Cr, V, Se, As, Cu, Sb, Mn, Na, Pb, Ti, Mg, Ba, and Zn;

Table 3. Indicatory elements for various major sources.

Indicatory elements	Source	Reference
Na, Sb, Mn, Fe, Cr, Cu, Ni, Se, V, and Zn	industrial emission	Tsai *et al.*, 2007; Zhang *et al.*, 2009; AEA, 2011; Bhangare *et al.*, 2011; Taiwo *et al.*, 2014
S, Cl, As, Se, and Pb	Smelting and coal combustion	Zhang *et al.*, 2009; Bhangare *et al.*, 2011
Zn, Cu, and Ba	Brake linings and tire tread wear	Garg *et al.*, 2000; Bozlaker *et al.*, 2013; Bozlaker *et al.*, 2014
Cu, Zn, Sb, V, Ni, Cr, Pb, Cd, and Cl	Vehicular emission	Cadle *et al.*, 1999; Sternbeck *et al.*, 2002; Fang *et al.*, 2006; Viana *et al.*, 2006; Pan *et al.*, 2013
Ni, V, and Cr	Oil fuel	AEA, 2011
K, Ba, and Cl	Biomass burning	Argyropoulos *et al.*, 2013; Wang *et al.*, 2016
V, Ni, Sb, and Cr	Aircraft and vehicle	Charlesworth *et al.*, 2011; Ren *et al.*, 2012
Mg, Al, Si, K, Ca, Ti, Ba, K, Mn, and Fe	Dust	Jiang *et al.*, 2018a

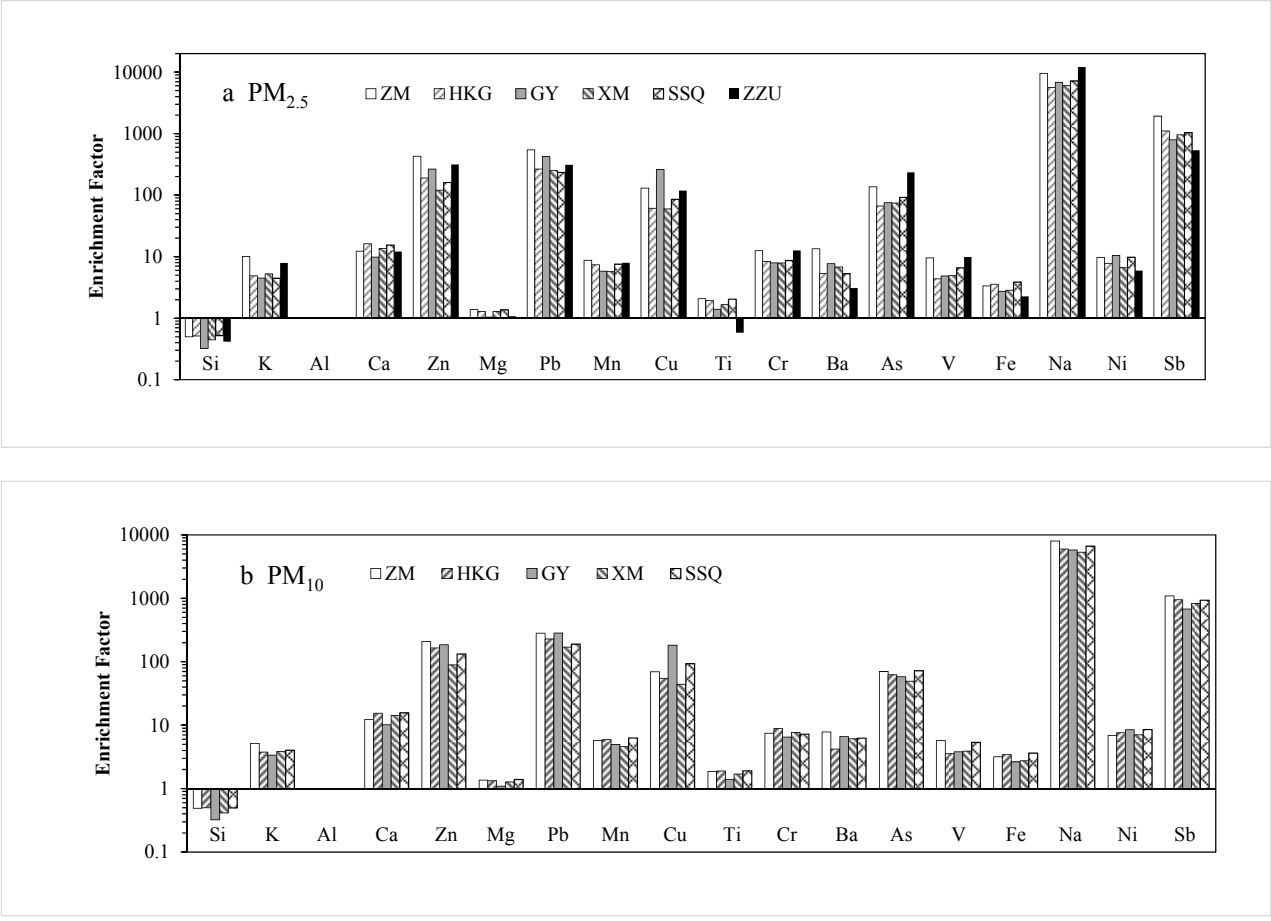

Fig. 5. Enrichment factors for elements among the sampling sites in Zhengzhou in 2016.

Cluster 2 contains partly or entirely crustal elements, i.e., Al, Fe, Si, Ca, K; other elements are distributed to Clusters 3 and 4 (if any). Similar clusters of elements exhibit good correlations, suggesting common sources (Sun *et al.*, 2014). The sources can be identified by fingerprint elements (Table 3). The results suggested that vehicular emission, industrial emission, coal combustion, and oil fuel were probable important sources of PM-bound elements in Zhengzhou. In addition, dust and biomass burning also affected elemental levels in PM.

Principal Component Analysis

In this study, PCA with varimax rotation was conducted for identifying the sources of elements in PM by using the software (SPSS 22.0), and the retention of principal components with eigenvalues greater than 1.0 was used to identify the main pollutant sources (Winner and Cass, 2001). Tables 5 and 6 present the PCA results of elements in $PM_{2.5}$ and PM_{10} in each sampling site, respectively. Elemental loadings higher than 0.6 are in bold and considered to be important.

Table 4. Correlation coefficients of elements in PM among the sampling sites in Zhengzhou in 2016 ($PM_{2.5}$: bottom left; PM_{10}: upper right).

ZM	Na	Mg	Al	Si	S	Cl	K	Ca	Ti	V	Ni	Cu	Zn	As	Se	Sb	Ba	Pb	Cr	Mn	Fe
Na	1	**.737****	.662**	.559**	.271*	**.735****	**.709****	.533**	.437**	.619**	.323*	.658**	.268*	0.245	.462**	.672**	.606**	.631**	.346**	.670**	.689**
Mg	**.702****	1	**.980****	**.914****	–0.044	.457**	**.763****	**.825****	.617**	**.720****	.455**	.642**	0.139	0.02	0.225	**.773****	**.737****	.527**	.564**	**.779****	**.909****
Al	.563**	**.957****	1	**.957****	–0.026	.420**	**.736****	**.841****	.669**	.683**	.506**	.624**	0.129	0.004	0.242	**.760****	**.700****	.497**	.578**	**.802****	**.937****
Si	.445**	**.824****	**.936****	1	–0.082	0.251	.531**	**.884****	**.717****	.584**	.527**	.455**	0.142	–0.073	0.181	.599**	.484**	.361**	.553**	**.806****	**.939****
S	.433**	–0.118	–0.189	–0.235	1	.689**	.299*	–0.052	0.199	–0.152	0.053	.413**	.362**	.646**	**.877****	0.208	0.085	.654**	0.11	.421**	0.193
Cl	**.711****	.304*	0.084	–0.154	.626**	1	**.796****	0.265	.333*	.430**	0.235	**.736****	.351**	.520**	**.805****	.669**	.607**	**.859****	0.249	.590**	.501**
K	.587**	.542**	.338*	0.012	.314*	**.836****	1	.443**	.369**	.675**	.314*	**.826****	0.138	.278*	.481**	**.892****	**.942****	**.743****	.447**	.605**	.650**
Ca	.508**	**.743****	**.806****	**.890****	–0.169	–0.072	–0.016	1	**.758****	.492**	.507**	.466**	.335*	–0.154	0.15	.591**	.403**	.405**	.529**	**.787****	**.869****
Ti	.409**	.613**	**.702****	**.785****	–0.117	–0.079	–0.038	**.761****	1	.320*	.401**	.405**	.339*	0.075	.360**	.432**	.286*	.391**	.388**	**.740****	**.764****
V	.566**	.455**	.327*	0.181	0.069	.516**	.521**	0.236	0.129	1	.431**	.494**	0	0.032	0.103	.647**	.674**	.419**	.401**	.452**	.604**
Ni	0.235	0.227	.328*	.408**	0.259	–0.021	–0.083	.404**	.354**	0.013	1	.391**	0.209	–0.087	0.245	.391**	0.234	.323*	.666**	.605**	.568**
Cu	.598**	.558**	.406**	0.162	.346**	**.711****	**.833****	0.183	0.121	.491**	0.175	1	0.257	0.261	.519**	**.752****	**.789****	**.764****	.542**	.630**	.591**
Zn	.462**	0.077	0.003	–0.014	.358**	.407**	0.201	0.128	0.096	.278*	0.151	.271*	1	0.183	.383**	0.225	0.083	.482**	0.198	.495**	.280*
As	.357**	0.014	–0.06	–0.128	.543**	.414**	.271*	–0.19	–0.08	–0.04	0.06	0.213	0.13	1	.650**	0.08	0.131	.580**	0.012	0.257	0.15
Se	.640**	0.195	0.092	0.01	**.828****	**.745****	.490**	0.035	0.071	0.197	.314*	.505**	.407**	.577**	1	.382**	0.234	**.772****	0.206	.597**	.449**
Sb	.656**	.591**	.441**	0.211	.312*	**.714****	**.802****	.272*	0.115	.629**	0.135	**.753****	.266*	0.205	.462**	1	**.859****	.670**	.509**	.643**	.684**
Ba	.396**	.534**	.364**	0.031	0.102	.632**	**.941****	–0.057	–0.054	.412**	–0.115	**.782****	0.093	0.183	.277*	**.726****	1	.596**	.432**	.470**	.542**
Pb	**.718****	.339**	0.16	–0.054	.669**	.889**	**.778****	–0.002	–0.022	.481**	0.1	**.760****	.535**	.525**	**.765****	**.748****	.631**	1	.424**	**.722****	.608**
Cr	.479**	.556**	.575**	.545**	0.082	0.21	0.242	.459**	.317*	0.133	.466**	.396**	0.158	0.152	.327*	.414**	0.188	.310*	1	.670**	.577**
Mn	**.833****	.620**	.560**	.562**	.398**	.448**	.300*	**.702****	.537**	.328*	.493**	.456**	.512**	0.225	.571**	.528**	0.141	.560**	.566**	1	**.923****
Fe	.629**	**.831****	**.912****	**.955****	–0.005	0.051	0.116	**.880****	**.787****	.282*	.456**	0.259	0.147	0.042	0.232	.342**	0.068	0.166	.606**	**.710****	1

* indicated significant correlation at the 0.05 level (bilateral); ** indicated significant correlation at the 0.01 level (bilateral).

Table 4. (*continued*).

HKG	Na	Mg	Al	Si	S	Cl	K	Ca	Ti	V	Ni	Cu	Zn	As	Se	Sb	Ba	Pb	Cr	Mn	Fe
Na	1	**.810****	**.743****	.679**	.430**	**.709****	**.880****	.613**	.636**	.689**	.274*	.471**	.526**	.399**	.588**	**.784****	**.744****	.644**	.266*	**.710****	.694**
Mg	**.891****	1	**.967****	**.947****	0.073	.329*	**.773****	**.900****	**.886****	**.720****	.493**	.361**	.388**	0.137	.281*	**.811****	.620**	.370**	.402**	**.846****	**.908****
Al	**.855****	**.985****	1	**.990****	0.028	0.242	**.743****	**.899****	**.937****	**.712****	.610**	.329*	.307*	0.13	0.245	**.793****	.567**	.301*	.463**	**.847****	**.939****
Si	**.847****	**.976****	**.997****	1	0.003	0.157	.677**	**.911****	**.958****	.669**	.652**	.300*	.306*	0.079	0.194	**.766****	.477**	0.246	.470**	**.853****	**.949****
S	0.004	–.286*	–.283*	–0.274	1	**.805****	.455**	0.107	0.153	0.097	–0.038	.358**	.625**	.578**	**.909****	.426**	.296*	**.798****	–0.109	.358**	0.169
Cl	0.181	–0.181	–0.228	–0.256	.699**	1	**.769****	0.232	0.236	.408**	–0.066	.565**	.645**	.596**	**.883****	.609**	**.709****	**.917****	0.072	.477**	.316*
K	**.714****	.605**	.584**	.548**	0.19	.539**	1	.657**	.687**	**.736****	.295*	.552**	.529**	.423**	.661**	**.853****	**.911****	**.743****	.352**	**.794****	**.765****
Ca	**.798****	**.958****	**.957****	**.950****	–0.255	–0.243	.520**	1	**.928****	.583**	.561**	.396**	.436**	0.105	0.247	**.837****	.471**	.347**	.467**	**.899****	**.931****
Ti	**.818****	**.962****	**.989****	**.989****	–0.241	–0.237	.557**	**.966****	1	.650**	.625**	.341*	.395**	0.162	.306*	**.800****	.463**	.348**	.465**	**.918****	**.978****
V	**.753****	**.823****	**.848****	**.831****	–0.163	0.012	**.702****	**.837****	**.858****	1	.366**	.284*	.299*	0.179	.290*	.601**	.671**	.395**	.427**	.635**	.689**
Ni	.690**	**.804****	**.815****	**.792****	–0.254	–0.051	.652**	**.753****	**.793****	.779**	1	0.227	0.252	–0.039	0.097	.417**	0.076	0.088	.635**	.569**	.626**
Cu	.284*	0.236	0.213	0.189	0.055	.300*	.467**	0.196	0.199	0.201	.424**	1	.677**	0.248	.428**	.608**	.491**	.699**	.379**	.551**	.416**
Zn	.399**	0.152	0.092	0.112	.390**	.399**	0.217	0.129	0.098	0.045	–0.025	.383**	1	.345**	.624**	.637**	.350**	**.769****	0.262	.629**	.470**
As	0.278	0.05	0.042	0.027	.578**	.588**	.350*	0.052	0.061	0.149	0.125	0.111	0.224	1	.684**	.384**	.322*	.657**	0.157	.308*	0.172
Se	0.166	–0.082	–0.094	–0.083	**.880****	.593**	0.209	–0.071	–0.062	–0.055	–0.076	0.217	.502**	.514**	1	.572**	.514**	**.888****	0.022	.509**	.350**
Sb	**.840****	**.852****	**.826****	**.800****	–0.066	0.198	**.823****	**.841****	**.814****	**.861****	**.740****	.398**	0.259	0.195	0.023	1	.658**	.670**	.431**	**.887****	**.845****
Ba	.548**	.558**	.532**	.487**	–0.044	.340*	**.911****	.485**	.500**	.634**	.670**	.438**	0.007	0.173	–0.034	**.740****	1	.630**	0.259	.561**	.555**
Pb	.384**	0.057	0.015	0.004	.696**	**.849****	.583**	0.033	0.024	0.146	0.057	.433**	.670**	.626**	.677**	.381**	.358*	1	0.225	.618**	.426**
Cr	.610**	**.747****	**.749****	**.749****	–0.19	–0.155	.474**	**.805****	**.765****	.681**	.624**	.427**	.349*	–0.098	0.028	**.739****	.431**	0.152	1	.517**	.515**
Mn	.686**	**.804****	**.808****	**.796****	–0.116	–0.103	.499**	**.801****	**.818****	.679**	**.775****	.546**	0.191	0.103	0.181	.661**	.426**	0.114	**.728****	1	**.958****
Fe	**.841****	**.964****	**.988****	**.987****	–0.206	–0.195	.586**	**.962****	**.996****	**.865****	**.787****	0.223	0.139	0.079	–0.024	**.830****	.507**	0.067	**.770****	**.829****	1

* indicated significant correlation at the 0.05 level (bilateral); ** indicated significant correlation at the 0.01 level (bilateral).

Table 4. (*continued*).

GY	Na	Mg	Al	Si	S	Cl	K	Ca	Ti	V	Ni	Cu	Zn	As	Se	Sb	Ba	Pb	Cr	Mn	Fe
Na	1	**.870****	**.839****	**.769****	.331**	**.734****	**.797****	**.757****	**.726****	**.834****	**.657****	.520**	.537**	.272*	**.667****	**.845****	.688**	.570**	.565**	**.699****	**.763****
Mg	.644**	1	**.914****	**.943****	0.078	.515**	**.747****	**.901****	**.867****	**.852****	.559**	.385**	.383**	0.124	.410**	**.843****	**.713****	.469**	.541**	**.740****	**.851****
Al	.626**	**.948****	1	**.934****	0.14	.656**	.647**	**.924****	**.956****	**.880****	**.695****	.504**	.541**	0.197	.480**	**.822****	.557**	.499**	**.707****	**.855****	**.927****
Si	.570**	**.951****	**.957****	1	0.06	.429**	.612**	**.932****	**.953****	**.854****	.580**	.331**	.379**	0.12	.333**	**.760****	.547**	.376**	.583**	**.824****	**.923****
S	.266*	0.132	0.237	0.088	1	.595**	.375**	0.108	0.142	.286*	.387**	0.188	.609**	**.763****	**.793****	.439**	0.177	.567**	.432**	.466**	.315*
Cl	.513**	.401**	.443**	.279*	.573**	1	.598**	.506**	.525**	**.616****	**.649****	.583**	**.758****	.516**	**.817****	**.733****	.420**	**.699****	.626**	**.619****	.592**
K	.409**	.546**	.421**	.346**	.411**	.577**	1	.523**	.515**	**.759****	.531**	.258*	.318*	0.248	.584**	**.799****	**.939****	.492**	.414**	.522**	.588**
Ca	.557**	**.898****	**.968****	**.941****	0.215	.330*	.307*	1	**.953****	**.816****	.575**	.450**	.524**	0.223	.410**	**.792****	.456**	.511**	.631**	**.842****	**.915****
Ti	.566**	**.907****	**.977****	**.966****	0.249	.339**	.335**	**.983****	1	**.841****	**.645****	.414**	.520**	0.22	.397**	**.757****	.428**	.443**	**.711****	**.892****	**.960****
V	.562**	**.842****	**.878****	**.859****	.309*	.375**	.482**	**.865****	**.883****	1	**.699****	.395**	.474**	0.198	.533**	**.840****	.623**	.505**	.625**	**.788****	**.853****
Ni	.494**	**.701****	**.798****	**.757****	.436**	.429**	.314*	**.780****	**.820****	**.780****	1	.432**	.545**	.273*	.500**	.612**	.371**	.464**	**.755****	.692**	**.704****
Cu	.515**	.508**	.593**	.439**	.332**	.567**	.295*	.568**	.520**	.471**	.480**	1	**.752****	0.165	.578**	.440**	0.198	.492**	.529**	.480**	.439**
Zn	.501**	.465**	.597**	.432**	**.705****	**.729****	.346**	.593**	.574**	.494**	.614**	**.775****	1	.604**	**.805****	.596**	0.173	**.800****	.666**	**.708****	.604**
As	.299*	.326*	.435**	.328*	.658**	.480**	.303*	.457**	.462**	.412**	.476**	.343**	.677**	1	.695**	.399**	0.092	**.724****	.394**	.449**	.337**
Se	.485**	.394**	.444**	.264*	**.783****	**.812****	.603**	.383**	.378**	.431**	.418**	.647**	**.834****	.636**	1	.639**	.408**	**.754****	.572**	.627**	.528**
Sb	.525**	**.825****	**.817****	**.748****	.435**	.545**	.666**	**.790****	**.778****	**.742****	.664**	.515**	.659**	.567**	.576**	1	.698**	**.691****	.641**	**.775****	**.794****
Ba	.332**	.468**	.320*	0.236	.356**	.445**	**.946****	0.221	0.233	.363**	0.197	.255*	.271*	.255*	.537**	.598**	1	.387**	.271*	.375**	.463**
Pb	.412**	.429**	.460**	.330**	.586**	.659**	.477**	.455**	.426**	.447**	.434**	.520**	**.793****	**.789****	**.741****	.696**	.431**	1	.514**	.575**	.528**
Cr	.563**	.692**	**.813****	**.713****	.523**	.489**	.306*	**.811****	**.823****	**.741****	**.855****	.586**	**.729****	.629**	.557**	.697**	0.234	.534**	1	**.804****	**.755****
Mn	.593**	**.837****	**.931****	**.874****	.447**	.463**	.387**	**.941****	**.950****	**.875****	**.846****	.597**	**.719****	.598**	.538**	**.801****	.292*	.542**	**.896****	1	**.953****
Fe	.569**	**.880****	**.958****	**.938****	.337**	.372**	.347**	**.971****	**.989****	**.876****	**.847****	.535**	.631**	.510**	.431**	**.783****	0.244	.463**	**.857****	**.975****	1

* indicated significant correlation at the 0.05 level (bilateral); ** indicated significant correlation at the 0.01 level (bilateral).

Table 4. (*continued*).

XM	Na	Mg	Al	Si	S	Cl	K	Ca	Ti	V	Ni	Cu	Zn	As	Se	Sb	Ba	Pb	Cr	Mn	Fe
Na	1	**.770****	**.701****	.685**	.248*	.518**	.634**	.425**	.569**	.590**	.254*	.372**	.273*	.427**	0.192	.580**	.497**	.377**	.403**	.598**	.605**
Mg	**.803****	1	**.964****	**.953****	0.127	.418**	**.726****	**.849****	**.903****	**.856****	.613**	.434**	.361**	.376**	0.214	**.870****	.526**	.433**	.628**	**.853****	**.876****
Al	**.736****	**.980****	1	**.967****	0.081	.361**	**.704****	**.839****	**.940****	**.875****	.675**	.398**	.324**	.317*	0.198	**.859****	.507**	.400**	.635**	**.850****	**.875****
Si	**.756****	**.969****	**.986****	1	0.027	0.226	.585**	**.865****	**.967****	**.898****	.666**	.263*	.285*	.247*	0.145	**.790****	.367**	.306*	.591**	**.869****	**.919****
S	–0.073	–.274*	–.311*	–.315*	1	**.768****	.325**	0.148	0.079	0.084	0.192	.547**	**.837****	**.830****	**.892****	.286*	0.161	**.830****	0.233	.290*	0.123
Cl	0.207	0.14	0.057	–0.029	.655**	1	**.765****	0.22	0.205	.263*	0.219	**.836****	.694**	**.810****	.682**	.590**	.668**	**.855****	.382**	.390**	.262*
K	.363**	.470**	.401**	.304*	.290*	**.839****	1	.459**	.511**	.559**	.410**	**.792****	.390**	.486**	.362**	**.863****	.935**	.654**	.536**	.586**	.549**
Ca	.598**	**.907****	**.912****	**.915****	–.346**	–0.076	0.23	1	**.928****	**.813****	**.741****	.284*	.461**	.353**	.281*	**.801****	0.221	.393**	.620**	**.815****	**.835****
Ti	**.737****	**.958****	**.982****	**.991****	–.307*	–0.038	.279*	**.937****	1	**.892****	**.753****	.251*	.363**	.290*	0.221	**.788****	.279*	.341**	.610**	**.875****	**.916****
V	.692**	**.810****	**.825****	**.822****	–0.2	0.115	.375**	.685**	**.796****	1	.691**	.260*	.338**	.299*	0.207	**.759****	.358**	.353**	.603**	**.823****	**.863****
Ni	.361**	.496**	.535**	.557**	–.320*	–.318*	–0.093	.556**	.584**	.471**	1	.281*	.444**	.276*	.362**	.656**	.251*	.442**	.578**	.671**	.670**
Cu	0.089	0.189	0.114	0.013	.336*	**.760****	**.814****	0.059	0.008	0.087	–0.085	1	.650**	.616**	.532**	.646**	**.746****	**.797****	.502**	.422**	.311*
Zn	0.065	0.067	0.035	0.034	**.703****	.524**	.292*	0.105	0.051	0.129	0.048	.485**	1	**.793****	**.852****	.495**	0.172	**.889****	.549**	.564**	.399**
As	.332*	0.22	0.164	0.133	**.733****	**.743****	.517**	0.114	0.148	0.225	–0.187	.472**	.697**	1	**.825****	.496**	.294*	**.848****	.387**	.476**	.332**
Se	–0.07	–0.133	–0.145	–0.156	**.866****	.575**	.279*	–0.167	–0.152	–0.029	–0.174	.294*	**.771****	**.712****	1	.382**	0.199	**.890****	.325**	.423**	.250*
Sb	.545**	**.707****	.630**	.561**	0.144	.674**	**.893****	.546**	.544**	.525**	0.119	**.765****	.368**	.523**	0.179	1	.696**	.628**	.678**	**.782****	**.765****
Ba	0.233	.319*	0.244	0.134	0.189	**.791****	**.954****	0.061	0.107	0.223	–0.164	**.801****	0.103	.354**	0.139	**.784****	1	.507**	.383**	.338**	.326**
Pb	0.08	0.077	0.025	–0.036	**.787****	**.840****	.642**	–0.017	–0.03	0.091	–0.195	**.711****	**.846****	**.837****	**.809****	.570**	.515**	1	.530**	.538**	.379**
Cr	0.252	.372**	.337*	.290*	0.128	.334*	.387**	.335*	.299*	0.22	.300*	.488**	.437**	.285*	0.18	.513**	.272*	.423**	1	**.783****	**.709****
Mn	**.726****	**.880****	**.880****	**.896****	0.042	0.194	.391**	**.829****	**.896****	**.741****	.486**	0.18	.410**	.430**	0.196	.641**	0.153	.314*	.496**	1	**.967****
Fe	**.767****	**.961****	**.972****	**.991****	–0.239	0.013	.319*	**.915****	**.990****	**.811****	.569**	0.038	0.113	0.194	–0.093	.582**	0.133	0.026	.327*	**.926****	1

* indicated significant correlation at the 0.05 level (bilateral); ** indicated significant correlation at the 0.01 level (bilateral).

Table 4. (*continued*).

SSQ	Na	Mg	Al	Si	S	Cl	K	Ca	Ti	V	Ni	Cu	Zn	As	Se	Sb	Ba	Pb	Cr	Mn	Fe
Na	1	**.789****	**.738****	**.700****	–0.034	.369**	.683**	.578**	**.701****	.602**	.472**	.388**	0.113	0.129	–0.025	.621**	.552**	.255*	.509**	.683**	**.745****
Mg	**.898****	1	**.973****	**.952****	–.319**	0.108	.687**	**.880****	**.927****	.635**	.655**	.453**	0.102	–0.061	–0.168	.642**	.530**	0.093	.630**	**.838****	**.917****
Al	**.841****	**.984****	1	**.985****	–.277*	0.086	.693**	**.835****	**.959****	.692**	.676**	.482**	0.111	–0.022	–0.131	.646**	.496**	0.102	.602**	**.860****	**.955****
Si	**.832****	**.975****	**.996****	1	–.286*	–0.008	.589**	**.851****	**.978****	.683**	.688**	.453**	0.122	–0.056	–0.13	.576**	.359**	0.033	.581**	**.866****	**.968****
S	–0.076	–.304*	–.319*	–.309*	1	.650**	0.117	–0.232	–.244*	0.07	0.097	0.231	.637**	.614**	**.809****	.315**	–0.088	**.767****	0.215	0.072	–0.136
Cl	0.239	0.039	–0.009	–0.015	.826**	1	.642**	0.042	0.021	0.17	0.202	.407**	.564**	.537**	.595**	.649**	.506**	**.895****	.447**	.326**	0.145
K	**.826****	**.828****	**.808****	**.791****	0.193	.521**	1	.446**	.555**	.525**	.441**	.509**	.251*	.241*	0.169	**.797****	**.877****	.566**	.564**	.625**	.631**
Ca	**.809****	**.960****	**.944****	**.940****	–.342**	–0.004	**.758****	1	**.862****	.476**	.691**	.421**	.285*	–0.113	–0.008	.582**	.251*	0.114	.677**	**.827****	**.829****
Ti	**.840****	**.965****	**.985****	**.992****	–.296*	–0.002	**.786****	**.940****	1	.656**	**.730****	.444**	0.159	0.003	–0.092	.604**	.321**	0.074	.606**	**.908****	**.978****
V	**.725****	.690**	.672**	.678**	0.072	.296*	**.713****	.624**	**.707****	1	.581**	.419**	0.214	0.109	0.086	.560**	.298*	0.198	.506**	.644**	.693**
Ni	**.721****	**.781****	**.774****	**.782****	–0.045	0.166	**.723****	**.776****	**.794****	.615**	1	.565**	.477**	0.162	0.159	.606**	0.187	.306*	.639**	**.799****	**.705****
Cu	.621**	.660**	.652**	.626**	0.128	.426**	**.794****	.600**	.616**	.439**	.558**	1	.481**	.252*	.285*	.550**	.344**	.457**	.502**	.581**	.498**
Zn	0.092	0.02	0.006	0.012	.661**	**.777****	.398**	0.049	0.02	0.052	0.2	.418**	1	.359**	**.718****	.444**	0.01	**.727****	.547**	.459**	0.233
As	0.153	0.005	–0.003	–0.017	.671**	.677**	.383**	–0.079	–0.026	0.214	0.125	.266*	.421**	1	.534**	.425**	0.084	.646**	.244*	0.224	0.058
Se	–0.074	–.262*	–.284*	–.272*	**.908****	**.838****	0.222	–.260*	–0.244	0.119	0.013	0.111	**.724****	.649**	1	.390**	–0.083	**.739****	.348**	0.209	0.006
Sb	**.790****	**.822****	**.799****	**.788****	0.159	.477**	**.927****	**.804****	**.793****	**.725****	**.789****	.678**	.358**	.375**	0.247	1	.575**	**.706****	**.712****	**.781****	.673**
Ba	.696**	.694**	.640**	.584**	–0.076	.282*	**.802****	.603**	.571**	.503**	.457**	**.713****	0.136	0.199	–0.071	.679**	1	.392**	.314**	.333**	.371**
Pb	0.171	0.026	–0.008	–0.021	**.832****	**.938****	.530**	0.003	–0.017	0.234	0.212	.415**	**.782****	**.750****	**.843****	.503**	.317*	1	.524**	.409**	0.188
Cr	.564**	.641**	.632**	.633**	0.183	.459**	**.783****	.665**	.651**	.529**	**.723****	.580**	.409**	.366**	.321*	**.832****	.507**	.527**	1	**.786****	.660**
Mn	**.793****	**.880****	**.891****	**.898****	0.003	.327*	**.887****	**.858****	**.915****	**.738****	**.841****	**.705****	.343**	0.212	0.093	**.901****	.587**	.325*	**.817****	1	**.937****
Fe	**.852****	**.960****	**.980****	**.987****	–0.225	0.071	**.823****	**.920****	**.994****	**.736****	**.806****	.649**	0.068	0.042	–0.181	**.820****	.595**	0.056	.681**	**.937****	1

* indicated significant correlation at the 0.05 level (bilateral); ** indicated significant correlation at the 0.01 level (bilateral).

Table 5. Varimax-rotated principal component loadings for elements in $PM_{2.5}$ among the sampling sites in Zhengzhou in 2016.

	ZM				HKG				GY		
	PC1	PC2	PC3	PC4	PC1	PC2	PC3	PC4	PC1	PC2	PC3
Na	0.52	0.52	0.37	0.44	**0.85**	0.28	0.21	0.10	0.54	0.30	0.30
Mg	**0.81**	0.55	–0.09	–0.02	**0.97**	–0.07	0.15	0.06	**0.89**	0.09	0.39
Al	**0.91**	0.35	–0.12	–0.10	**0.98**	–0.09	0.13	0.02	**0.94**	0.23	0.18
Si	**0.97**	0.02	–0.13	–0.05	**0.98**	–0.09	0.08	0.02	**0.97**	0.04	0.15
S	–0.14	0.15	**0.84**	0.30	–0.20	**0.91**	–0.05	–0.01	0.05	**0.84**	0.14
Cl	–0.09	**0.75**	0.47	0.35	–0.23	**0.78**	0.50	0.13	0.18	**0.72**	0.39
K	0.02	**0.96**	0.19	0.03	0.52	0.34	**0.74**	0.14	0.21	0.27	**0.92**
Ca	**0.92**	–0.01	–0.14	0.21	**0.97**	–0.07	0.06	0.05	**0.95**	0.22	0.06
Ti	**0.82**	–0.08	–0.07	0.13	**0.99**	–0.06	0.09	0.01	**0.97**	0.21	0.07
V	0.17	0.61	–0.20	0.50	**0.84**	0.02	0.36	–0.06	**0.86**	0.21	0.24
Ni	0.53	–0.20	0.42	0.05	**0.76**	–0.11	0.43	0.11	**0.79**	0.38	0.00
Cu	0.21	**0.82**	0.26	0.10	0.15	0.11	0.38	**0.81**	0.44	0.56	0.10
Zn	0.05	0.11	0.24	**0.80**	0.16	0.56	–0.22	**0.62**	0.40	**0.87**	0.04
As	–0.06	0.17	**0.76**	–0.13	0.10	**0.76**	0.20	–0.24	0.29	**0.77**	0.01
Se	0.11	0.32	**0.82**	0.27	0.00	**0.87**	–0.17	0.19	0.17	**0.85**	0.38
Sb	0.25	**0.82**	0.18	0.20	**0.80**	0.14	0.46	0.17	**0.68**	0.41	0.46
Ba	0.01	**0.94**	0.03	–0.15	0.43	0.06	**0.84**	0.11	0.12	0.22	**0.93**
Pb	0.02	**0.70**	0.56	0.37	0.04	**0.85**	0.31	0.32	0.25	**0.78**	0.26
Cr	**0.64**	0.21	0.33	–0.10	**0.77**	–0.07	0.03	0.47	**0.75**	0.53	–0.02
Mn	**0.68**	0.20	0.41	0.48	**0.81**	0.02	0.06	0.35	**0.88**	0.42	0.08
Fe	**0.96**	0.09	0.07	0.10	**0.99**	–0.02	0.09	0.04	**0.94**	0.29	0.06
% of variance	30.7	26.6	16.2	9.2	48.9	19.4	12.0	8.0	45.0	26.1	12.8

Table 5. (*continued*).

	XM				SSQ	
	PC1	PC2	PC3	PC4	PC1	PC2
Na	**0.81**	0.07	0.17	–0.14	**0.89**	0.05
Mg	**0.95**	–0.07	0.25	0.10	**0.98**	–0.14
Al	**0.96**	–0.09	0.16	0.11	**0.97**	–0.16
Si	**0.98**	–0.08	0.05	0.09	**0.97**	–0.17
S	–0.25	**0.90**	0.15	–0.09	–0.18	**0.92**
Cl	–0.01	0.58	**0.77**	–0.09	0.16	**0.94**
K	0.28	0.23	**0.92**	–0.01	**0.89**	0.39
Ca	**0.90**	–0.09	0.02	0.24	**0.94**	–0.16
Ti	**0.98**	–0.07	0.02	0.12	**0.97**	–0.16
V	**0.85**	0.03	0.13	–0.02	**0.75**	0.16
Ni	0.54	–0.17	–0.26	0.56	**0.84**	0.09
Cu	–0.03	0.28	**0.85**	0.33	**0.72**	0.31
Zn	0.07	**0.87**	0.09	0.37	0.13	**0.80**
As	0.22	**0.84**	0.32	–0.12	0.10	**0.77**
Se	–0.10	**0.93**	0.06	0.01	–0.13	**0.93**
Sb	0.53	0.20	**0.77**	0.16	**0.89**	0.36
Ba	0.09	0.05	**0.97**	–0.06	**0.71**	0.15
Pb	–0.01	**0.84**	0.49	0.15	**0.16**	**0.96**
Cr	0.23	0.22	0.32	**0.76**	**0.74**	0.41
Mn	**0.90**	0.30	0.08	0.22	**0.94**	0.20
Fe	**0.98**	–0.01	0.05	0.12	**0.98**	–0.08
% of variance	40.8	21.6	21.0	6.7	56.4	26.4

At ZM sampling site (rural site), for $PM_{2.5}$, Factor 1 accounts for 31% of the total variance of the data, with high loadings of Mg, Al, Si, Ca, Ti, Cr, Mn, and Fe, representing contributions from dust (Jiang *et al.*, 2018a) and industrial emission (Taiwo *et al.*, 2014); Factor 2 accounts for 27% of the total variance in the dataset, with high loadings of Cl, K, Cu, Sb, Ba, and Pb, which are representative of biomass burning and vehicular emission

Table 6. Varimax-rotated principal component loadings for elements in PM_{10} among the sampling sites in Zhengzhou in 2016.

	ZM			HKG			GY			XM			SSQ		
	PC1	PC2	PC3	PC1	PC2	PC3	PC1	PC2	PC3	PC1	PC2	PC3	PC1	PC2	PC3
Na	0.40	**0.64**	0.32	**0.77**	0.50	0.06	**0.62**	0.34	**0.60**	0.52	0.11	0.53	**0.65**	0.03	0.53
Mg	**0.70**	**0.67**	–0.03	**0.90**	0.11	0.34	**0.78**	0.05	0.57	**0.87**	0.08	0.42	**0.91**	–0.15	0.36
Al	**0.76**	**0.61**	–0.03	**0.89**	0.03	0.43	**0.90**	0.18	0.36	**0.90**	0.05	0.38	**0.92**	–0.12	0.32
Si	**0.87**	0.38	–0.09	**0.84**	–0.02	0.51	**0.89**	0.00	0.38	**0.95**	–0.01	0.23	**0.95**	–0.15	0.18
S	–0.02	0.01	**0.94**	–0.02	**0.90**	–0.02	–0.05	**0.87**	0.17	–0.02	**0.95**	0.10	–0.18	**0.91**	–0.03
Cl	0.12	**0.60**	**0.73**	0.32	**0.91**	–0.14	0.40	**0.72**	0.32	0.08	**0.71**	**0.65**	0.02	**0.76**	0.56
K	0.25	**0.90**	0.30	**0.79**	0.56	0.09	0.32	0.27	**0.89**	0.41	0.26	**0.85**	0.49	0.26	**0.80**
Ca	**0.90**	0.27	–0.04	**0.74**	0.10	0.56	**0.91**	0.14	0.26	**0.92**	0.19	0.03	**0.91**	–0.03	0.02
Ti	**0.80**	0.10	0.21	**0.77**	0.10	0.55	**0.95**	0.14	0.21	**0.97**	0.08	0.10	**0.96**	–0.09	0.14
V	0.35	**0.75**	–0.12	**0.80**	0.16	0.11	**0.74**	0.22	0.52	**0.90**	0.07	0.19	**0.69**	0.11	0.20
Ni	**0.66**	0.14	0.06	0.28	–0.07	**0.81**	**0.63**	0.40	0.20	**0.76**	0.26	–0.01	**0.81**	0.28	–0.05
Cu	0.31	**0.71**	0.41	0.17	**0.60**	0.40	0.48	0.48	–0.06	0.13	0.57	**0.70**	0.52	0.41	0.19
Zn	0.39	–0.14	0.52	0.13	**0.74**	0.44	0.46	**0.82**	–0.06	0.30	**0.91**	0.04	0.30	**0.82**	–0.16
As	–0.15	0.12	**0.75**	0.09	**0.69**	–0.03	0.03	**0.83**	0.05	0.20	**0.86**	0.24	–0.02	**0.69**	0.16
Se	0.18	0.18	**0.90**	0.21	**0.91**	0.01	0.23	**0.87**	0.31	0.14	**0.94**	0.04	–0.01	**0.89**	–0.11
Sb	0.39	**0.80**	0.19	**0.68**	0.50	0.41	0.61	0.42	0.58	**0.73**	0.28	0.54	**0.61**	0.50	0.49
Ba	0.18	**0.93**	0.09	**0.74**	0.47	–0.16	0.24	0.09	**0.92**	0.18	0.10	**0.94**	0.22	0.02	**0.92**
Pb	0.29	0.51	**0.73**	0.25	**0.94**	0.13	0.30	**0.77**	0.26	0.24	**0.87**	0.37	0.10	**0.90**	0.36
Cr	**0.61**	0.30	0.09	0.24	0.05	**0.69**	**0.70**	0.50	0.01	**0.65**	0.32	0.22	**0.70**	0.44	0.14
Mn	**0.82**	0.30	0.44	**0.68**	0.39	0.57	**0.82**	0.44	0.15	**0.88**	0.31	0.16	**0.92**	0.28	0.15
Fe	**0.84**	0.43	0.20	**0.79**	0.17	0.55	**0.89**	0.28	0.25	**0.93**	0.12	0.16	**0.95**	0.01	0.20
% of variance	30.5	28.2	20.7	37.2	28.6	16.8	40.5	25.6	17.8	42.7	25.9	18.3	43.8	24.1	14.1

(Fang *et al.*, 2006; Pan *et al.*, 2013); Factor 3 (16%) is coal combustion (Bhangare *et al.*, 2011), with a high content of S, As, and Se; Factor 4 (9%) is dominated by Zn, which is reported to originate primarily from the industrial emission (AEA, 2011). For PM_{10}, Factor 1 accounts for 31% of the total variance, with high loadings of Mg, Al, Si, Ca, Ti, Ni, Cr, Mn, and Fe that came from dust and industrial emission (Taiwo *et al.*, 2014; Jiang *et al.*, 2018a); Factor 2 accounts for 28% of the total variance in the data and has high loadings of Na, Mg, Al, Cl, K, V, Cu, Sb, and Ba, suggesting that dust (Jiang *et al.*, 2018a) and vehicular emission (Charlesworth *et al.*, 2011) are the major contributors; high loadings of S, Cl, As, Se, and Pb are shown on Factor 3 (21%), considered to originate from coal combustion (Bhangare *et al.*, 2011).

At the HKG sampling site (traffic site), for $PM_{2.5}$, 49% of the total variance was observed in Factor 1, contributed by dust (Jiang *et al.*, 2018a) and traffic emission, i.e., aircraft and vehicle sources (Charlesworth *et al.*, 2011; Ren *et al.*, 2012), because of the high loadings of Na, Mg, Al, Si, Ca, Ti, V, Ni, Sb, Cr, Mn, and Fe; Factor 2, with a high content of S, Cl, As, Se, and Pb, represents the contribution of coal combustion (Bhangare *et al.*, 2011); Factor 3 (12%), with high loadings of K and Ba, represents biomass burning (Argyropoulos *et al.*, 2013) in view of Cl loading; and Factor 4 (8%), with a high content of Cu and Zn, represents vehicular emission (Viana *et al.*, 2006). For PM_{10}, Factor 1 (37%) is commonly related to dust (Jiang *et al.*, 2018a) and industrial emission (Taiwo *et al.*, 2014), characterized by high loads of Na, Mg, Al, Si, K, Ca, Ti, V, Ni, Sb, Ba, Mn, and Fe; Factor 2 (29%) is identified as coal combustion (Bhangare *et al.*, 2011) and industrial emission (AEA, 2011), with high loadings of S, Cl, Cu, As, Se, and Pb; and Factor 3 (17%), with a high content of Ni and Cr, represents oil fuel (AEA, 2011).

At the GY sampling site (urban site), for $PM_{2.5}$, Factor 1 shows 45% of the total variance and contributions by dust (Jiang *et al.*, 2018a) and vehicular emission (Charlesworth *et al.*, 2011) due to high loadings of Mg, Al, Si, Ca, Ti, V, Ni, Sb, Cr, Mn, and Fe; Factor 2, with high loadings of S, Cl, Zn, As, Se, and Pb, shows 26% of the total variance and represents the coal combustion (Bhangare *et al.*, 2011) and industrial emission (AEA, 2011); Factor 3 (13%) represents biomass burning (Argyropoulos *et al.*, 2013), with high loadings of K and Ba. For PM_{10}, Factor 1 explains 40% of the total variance, with a high content of Na, Mg, Al, Si, Ca, Ti, V, Ni, Cr, Mn, and Fe, representing dust (Jiang *et al.*, 2018a) and industrial emission sources (Taiwo *et al.*, 2014); Factor 2 (26%) has high loadings of S, Cl, Zn, As, Se, and Pb, which originated from coal combustion (Bhangare *et al.*, 2011) and industrial emission (AEA, 2011); and Factor 3 (18%) is strongly correlated with Na, K, and Ba and identified as biomass burning (Argyropoulos *et al.*, 2013; Wang *et al.*, 2016).

Given limited space, the details of PCA results in the other two urban sites are not shown with similar indicators. At the XM sampling site, for $PM_{2.5}$, Factor 1 (dust and vehicular emissions), Factor 2 (coal combustion and industrial emission), Factor 3 (biomass burning and vehicular emission), and Factor 4 (industrial emission) contribute 41%, 22%, 21%, and 7% of the variance, respectively; for PM_{10}, Factor 1 (dust and vehicular emissions), Factor 2 (coal combustion and industrial emission), and Factor 3 (biomass burning and industrial emission) contribute 43%, 26%, and 18% of the variance, respectively. At the SSQ sampling site, for $PM_{2.5}$, Factor 1 (dust and vehicular emission) and Factor 2 (coal combustion and industrial emission) account for 56% and 26% of the variance, respectively; for PM_{10}, Factor 1 (dust and vehicular emission), Factor 2 (coal combustion and industrial emission), and Factor 3 (biomass burning) contribute 44%, 24%, and 14% of the variance, respectively.

In the comparison of the source identification results among the five sites, the source contributions were found to be consistent with the category of sites. For example, ZM site is the rural site with low traffic effect. The main results included relatively high contributions of biomass burning, which is attributed to the use of straw as fuel for cooking and heating in winter, dust emission, and poor dust control measures in the country. HKG site is located near Xinzheng International Airport, and therefore, its traffic sources (i.e., aircraft and vehicles) contribute high proportion. SSQ site is an urban site with high traffic and is also affected highly by vehicle emission. Moreover, for comparison of $PM_{2.5}$ and PM_{10} sources, in brief, combustion sources, including coal combustion, vehicular emission, and biomass burning, played more important roles in elements in $PM_{2.5}$, whereas dust source contributed more to PM_{10}-bound elements.

Health Risks Posed by Toxic Elements

The health risk values, including CR, HQ, and HI, of toxic elements in $PM_{2.5}$ and PM_{10} through the inhalation, dermal absorption, and daily intake pathways are calculated in this study. For CR, $1 \times 10^{-6} < CR < 1 \times 10^{-4}$ indicates a tolerable risk for regulatory purposes, and $CR > 1 \times 10^{-4}$ indicates intolerable risk (U.S. EPA, 1989). Moreover, for noncarcinogenic risk, $HQ > 1$ and $HI > 1$ suggests a significant risk of a single element and total toxic elements (U.S. EPA, 1989). The relative detailed data of health risk evaluation from toxic elements in PM through the three exposure pathways are presented in Tables S1–S3 in Supplemental Materials, and the carcinogenic and noncarcinogenic risks among the sampling sites in Zhengzhou are exhibited in Tables 7, S4 and S5. Meanwhile, the total CR and HQ of toxic elements in $PM_{2.5}$ and PM_{10} are summarized in Fig. 6.

Overall, the CR values of As, Pb, and Ni were all higher than 1×10^{-6}, especially for As ($PM_{2.5}$: 1.2×10^{-4}–2.9×10^{-4}; PM_{10}: 1.0×10^{-4}–3.2×10^{-4}) and Ni ($PM_{2.5}$: 6.8×10^{-5}–1.9×10^{-4}; PM_{10}: 6.3×10^{-5}–1.8×10^{-4}), with CR values exceeding 1×10^{-4}, respectively. This result suggested that As and Ni caused intolerable risks and Pb showed tolerable risk in $PM_{2.5}$ and PM_{10} in Zhengzhou. According to the previous study (AEA, 2011), metal production, and public electricity and heat production are the major sources of As; combustion of heavy fuel oil is the major source of Ni. Therefore, the local regulatory agency should strengthen

Table 7. Carcinogenic and noncarcinogenic risks for each element in $PM_{2.5}$ and PM_{10} through the daily intake pathway among the sampling sites in Zhengzhou.

(a) ZM

Toxic elements	$PM_{2.5}$				PM_{10}			
	Carcinogenic risk		Non-Carcinogenic risk		Carcinogenic risk		Non-Carcinogenic risk	
	Children	Adults	Children	Adults	Children	Adults	Children	Adults
V			3.28E-01	4.16E-02			2.47E-01	3.14E-02
Cu			9.01E-02	1.15E-02			6.97E-02	8.86E-03
As	2.61E-04	1.33E-04	7.15E+00	9.08E-01	2.05E-04	1.04E-04	5.61E+00	7.13E-01
Mn			3.17E-01	4.03E-02			2.90E-01	3.68E-02
Zn			1.43E-01	1.82E-02			9.70E-02	1.23E-02
Pb	9.77E-06	4.97E-06	4.05E+00	5.15E-01	7.18E-06	3.65E-06	2.97E+00	3.78E-01
Ni	6.69E-05	3.40E-05	4.41E-02	5.61E-03	6.16E-05	3.13E-05	4.06E-02	5.17E-03
Sb			1.06E+01	1.34E+00			8.78E+00	1.12E+00
HI			1.41E+01	8.97E-01			1.81E+01	2.30E+00

(b) HKG

Toxic elements	$PM_{2.5}$				PM_{10}			
	Carcinogenic risk		Non-Carcinogenic risk		Carcinogenic risk		Non-Carcinogenic risk	
	Children	Adults	Children	Adults	Children	Adults	Children	Adults
V			2.05E-01	2.61E-02			1.52E-01	1.93E-02
Cu			8.55E-02	1.09E-02			6.77E-02	8.61E-03
As	1.92E-04	9.77E-05	5.26E+00	6.69E-01	1.69E-04	8.59E-05	4.63E+00	5.89E-01
Mn			4.92E-01	6.26E-02			3.06E-01	3.88E-02
Zn			9.39E-02	1.19E-02			7.36E-02	9.35E-03
Pb	7.61E-06	3.87E-06	3.15E+00	4.01E-01	6.05E-06	3.08E-06	2.51E+00	3.19E-01
Ni	7.72E-05	3.93E-05	5.09E-02	6.47E-03	7.68E-05	3.90E-05	5.06E-02	6.44E-03
Sb			8.86E+00	1.13E+00			7.28E+00	9.26E-01
HI			1.82E+01	2.31E+00			1.51E+01	1.92E+00

(c) GY

Toxic elements	$PM_{2.5}$				PM_{10}			
	Carcinogenic risk		Non-Carcinogenic risk		Carcinogenic risk		Non-Carcinogenic risk	
	Children	Adults	Children	Adults	Children	Adults	Children	Adults
V			2.35E-01	2.99E-02			2.06E-01	2.62E-02
Cu			3.57E-01	4.54E-02			2.93E-01	3.72E-02
As	2.64E-04	1.34E-04	7.23E+00	9.19E-01	2.20E-04	1.12E-04	6.02E+00	7.66E-01
Mn			3.52E-01	4.48E-02			3.43E-01	4.37E-02
Zn			1.25E-01	1.59E-02			1.01E-01	1.29E-02
Pb	1.46E-05	7.45E-06	6.07E+00	7.72E-01	1.08E-05	5.48E-06	4.47E+00	5.68E-01
Ni	1.10E-04	5.61E-05	7.28E-02	9.26E-03	1.03E-04	5.23E-05	6.78E-02	8.62E-03
Sb			7.00E+00	8.90E-01			6.55E+00	8.33E-01
HI			2.14E+01	2.73E+00			1.81E+01	2.30E+00

(b) SSQ

Toxic elements	$PM_{2.5}$				PM_{10}			
	Carcinogenic risk		Non-Carcinogenic risk		Carcinogenic risk		Non-Carcinogenic risk	
	Children	Adults	Children	Adults	Children	Adults	Children	Adults
V			3.03E-01	3.85E-02			3.41E-01	4.33E-02
Cu			9.62E-02	1.22E-02			1.41E-01	1.79E-02
As	2.68E-04	1.36E-04	7.33E+00	9.32E-01	2.97E-04	1.51E-04	8.14E+00	1.03E+00
Mn			3.71E-01	4.72E-02			4.13E-01	5.25E-02
Zn			6.71E-02	8.53E-03			7.94E-02	1.01E-02
Pb	5.68E-06	2.89E-06	2.36E+00	3.00E-01	6.62E-06	3.37E-06	2.74E+00	3.49E-01
Ni	8.06E-05	4.10E-05	5.31E-02	6.76E-03	9.74E-05	4.95E-05	6.42E-02	8.16E-03
Sb			7.51E+00	9.55E-01			9.03E+00	1.15E+00
HI			1.81E+01	2.30E+00			2.09E+01	2.66E+00

Table 7. (*continued*).

(e) XM

Toxic elements	$PM_{2.5}$				PM_{10}			
	Carcinogenic risk		Non-Carcinogenic risk		Carcinogenic risk		Non-Carcinogenic risk	
	Children	Adults	Children	Adults	Children	Adults	Children	Adults
V			2.50E-01	3.18E-02			2.32E-01	2.95E-02
Cu			8.13E-02	1.03E-02			6.78E-02	8.62E-03
As	2.16E-04	1.10E-04	5.92E+00	7.53E-01	1.79E-04	9.11E-05	4.91E+00	6.24E-01
Mn			3.29E-01	4.19E-02			3.00E-01	3.81E-02
Zn			6.16E-02	7.83E-03			4.66E-02	5.93E-03
Pb	7.47E-06	3.80E-06	3.10E+00	3.94E-01	5.45E-06	2.77E-06	2.26E+00	2.87E-01
Ni	1.07E-04	5.46E-05	7.09E-02	9.01E-03	9.15E-05	4.65E-05	6.04E-02	7.67E-03
Sb			7.46E+00	9.49E-01			8.05E+00	1.02E+00
HI			1.73E+01	2.20E+00			1.59E+01	2.02E+00

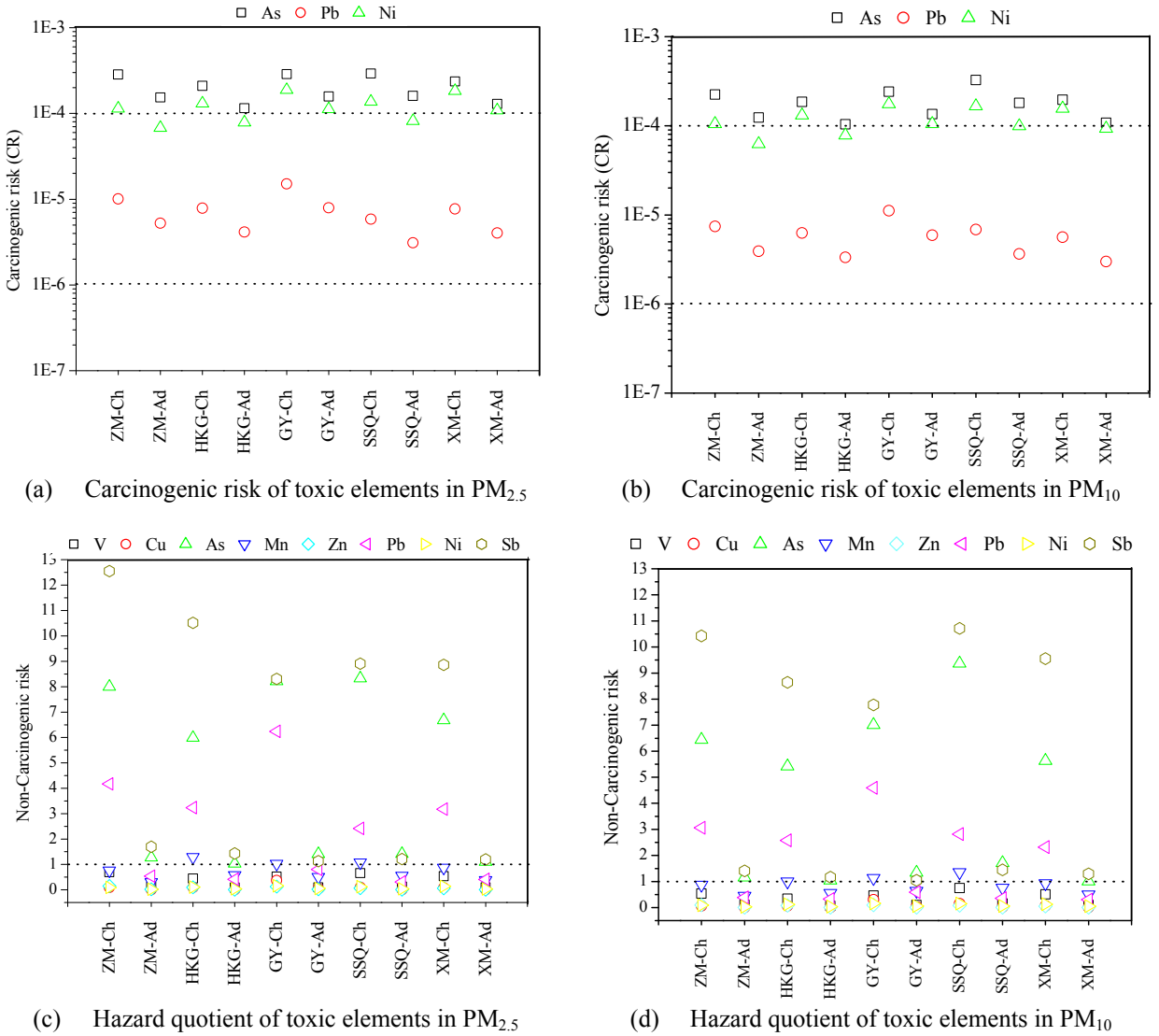

(a) Carcinogenic risk of toxic elements in $PM_{2.5}$

(b) Carcinogenic risk of toxic elements in PM_{10}

(c) Hazard quotient of toxic elements in $PM_{2.5}$

(d) Hazard quotient of toxic elements in PM_{10}

Fig. 6. Carcinogenic risk and hazard quotient of toxic elements in $PM_{2.5}$ and PM_{10} among the sampling sites in Zhengzhou in 2016.

management and control of coal-fired power plant and nonroad-mobile source emission to reduce As and Ni levels. The noncarcinogenic risks of As ($PM_{2.5}$: 1.03–8.33; PM_{10}: 1.01–9.37), Pb ($PM_{2.5}$: 0.31–6.24; PM_{10}: 0.30–4.59), and Sb ($PM_{2.5}$: 1.13–12.55; PM_{10}: 1.05–10.71) were higher than the threshold value, i.e., HQ = 1, indicating significant

risks. In general, for comparison with adults, children are more sensitive, with higher CR and HQ values.

Among the three exposure pathways, the daily intake is the limiting one. Generally, the highest CR of As, Pb, and Ni existed through the daily intake pathway, especially for As, with CR values ranging from 9.8×10^{-5} to 2.7×10^{-4} in $PM_{2.5}$ and from 8.6×10^{-5} to 3.0×10^{-4} in PM_{10}. The noncarcinogenic risk of all toxic elements, i.e., HI, was also the highest through the daily intake pathway, with the values ranging from 0.9 to 21.4 in $PM_{2.5}$ and from 1.9 to 18.1 in PM_{10}, which are far beyond the limit (HI = 1). Moreover, in this pathway, Sb, As, and Pb exhibited high risks, with HQ values all exceeding 1 for children, thereby also indicating significant risks. By contrast, CR and HQ values from toxic elements in PM through inhalation and dermal absorption exposure were relatively low. However, significant noncarcinogenic risks still existed because of HI > 1, especially for children.

For comparison among the five sites, the health risks differed with various elemental concentrations. In general, the total CR values from As, Pb, and Ni in $PM_{2.5}$ ranged from 3.5×10^{-4} (HKG) to 4.9×10^{-4} (GY) and 2.0×10^{-4} (HKG) to 2.8×10^{-4} (GY) for children and adults, respectively; the CR values in PM_{10} varied from 3.2×10^{-4} (HKG) to 5.0×10^{-4} (SSQ) and 1.9×10^{-4} (HKG) to 2.8×10^{-4} (SSQ) for children and adults, respectively. These results demonstrated intolerable CR from the three elements in PM at all the sites in Zhengzhou and thus should be given more attention. Moreover, the relatively obvious differences of CR at the sites, with values, i.e., the average ratio of difference between the lowest and highest risk, of 29% and 35% for $PM_{2.5}$ and PM_{10}. For noncarcinogenic risks, all total HI (i.e., $\sum$HI) of the sites were higher than 1, suggesting significant risks. For $PM_{2.5}$, the total HI values ranged from 16.6 (ZM) to 24.9 (GY) and 2.0 (ZM) to 4.1 (GY) for children and adults, with difference ratios of 34% and 51%, respectively. For PM_{10}, the total HI values were in the range of 18.2 (HKG)–25.4 (SSQ) and 3.3 (HKG)–4.5 (SSQ) for children and adults, respectively, both with difference ratios of 28%. Therefore, data at multiple sites are necessary for health risk assessment in the study area, especially for a large region.

Source Regions of PM and Toxic Elements

Fig. 7 shows the 48-h back trajectories of air masses arriving in Zhengzhou during the sampling periods, with 1140 transport trajectories. Obviously, four types of air mass clusters influenced the pollution levels of the sampling site. Two northwestern airflows with long trajectories occurred. The first one was mainly from Kazakhstan, Xinjiang, or Gansu, passing through the northern part of Qinghai, Shaanxi, Shanxi, and Northwestern Henan. The second airflow came from Russia, Mongolia, or Inner Mongolia, then by way of the Beijing-Tianjin-Hebei region and northern Henan. These areas, i.e., Mongolia, Inner Mongolia, Xinjiang, Gansu, and Shaanxi, were commonly covered by the Gobi Desert and grasslands. The long-range transport brought the mineral aerosols, mixing with the local emission and aggravating PM, especially crustal materials and pollution levels, and changing the ratio of Ca to Al (Zhang *et al.*, 2003), used to determine source area of dust, in the PM samples in this study area. Beijing-Tianjin-Hebei, characterized by huge consumption of coal and coal combustion as the predominant source of aerosols (Yao *et al.*, 2009), is always one of the most deteriorated regions in China (Tao *et al.*, 2016). Therefore, the second direction airflow probably increased the PM and elements relative to coal burning, i.e., S, Cl, As, Se, and Pb (Bhangare *et al.*, 2011) concentrations, especially in winter, i.e., high emission season because of extra coal consumption for central heating, including the local emission in Zhengzhou and the emission from the airflow passing regions. The medium to long distance transport covered the eastern regions of Zhengzhou, i.e., the Yellow Sea, Jiangsu, Northern Anhui,

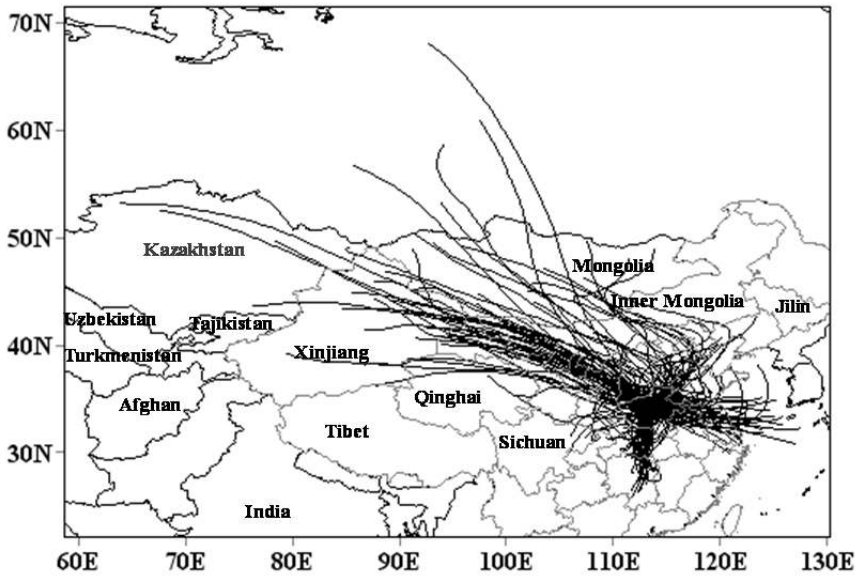

Fig. 7. Forty-eight-hour back trajectories of air masses arriving at SSQ site in Zhengzhou in 2016.

Southern Shandong, and Eastern Henan; these inland areas featured flourishing agriculture (Kang *et al.*, 2016). Hence, these trajectories from the east likely influenced the pollution level of PM, Na, Cl, and elements emitted from biomass burning, i.e., K and Ba (Argyropoulos *et al.*, 2013; Wang *et al.*, 2016), especially in harvest season. The short-distance transport from the southern areas of Zhengzhou covered Hunan, Hubei, and southern Henan. Generally, these regions present mitigating PM levels (Tao *et al.*, 2016), suggesting possible decreasing PM and elemental values in this study region due to dilution function.

In this study, source regions of PM_{10}, $PM_{2.5}$, and As, with the highest CR, were analyzed by PSCF model (Fig. 8). Generally, the potential source areas of the pollutants are almost distributed in the range of the surrounding regions of Zhengzhou in Henan Province. For $PM_{2.5}$, the northwestern and southeastern regions of Zhengzhou, i.e., Jiyuan, Jiaozuo, Xuchang, and Zhoukou, were likely potential source areas, with WPSCF values higher than 0.6. Moreover, the spatial source distributions of $PM_{2.5}$-bound As were confined in Jiyuan, Jiaozuo, Xinxiang, Anyang, and Kaifeng, which are the main industrial cities in Henan, with WPSCF values over 0.4. According to previous studies (AEA, 2011; Bhangare *et al.*, 2011), industrial production (e.g., metal production as well as public electricity and heat production) and coal combustion are the major sources of As. Therefore, the relative activities in the five industrial cities influenced the pollution levels of $PM_{2.5}$-bound As in Zhengzhou. For PM_{10}, the potential source area was in the southwestern areas of Zhengzhou, mainly including Pingdingshan and Nanyang (WPSCF values above 0.4). Pingdingshan is the largest coal-producing city in Henan, with raw coal products amounting to 34.0 Mt in 2016 (Bureau of Statistics of Pingdingshan, 2017). Coal mining processes emitted huge amounts of coarse particles and accompanied with south air trajectories, the air mass carried a large amount of particles, thereby influencing the PM_{10} concentration in Zhengzhou. Nanyang is a large agricultural city in Henan, with grain, oil-bearing crops, flue-cured tobacco, vegetables and edible fungus, and fruit outputs of 6.4, 1.4, 0.1, 10.5, and 1.6 Mt in 2016 (Bureau of Statistics of Henan Province, 2017). Agricultural activities and bare soil increased PM_{10} levels in Zhengzhou when the south winds form. The WPSCF values of PM_{10}-bound As, which are generally less than those of $PM_{2.5}$-bound As, showed similar spatial distributions in fine particles due to the industries located in the surrounding cities. For comparison, fine particles with higher WPSCF values are more easily transmitted than coarse particles.

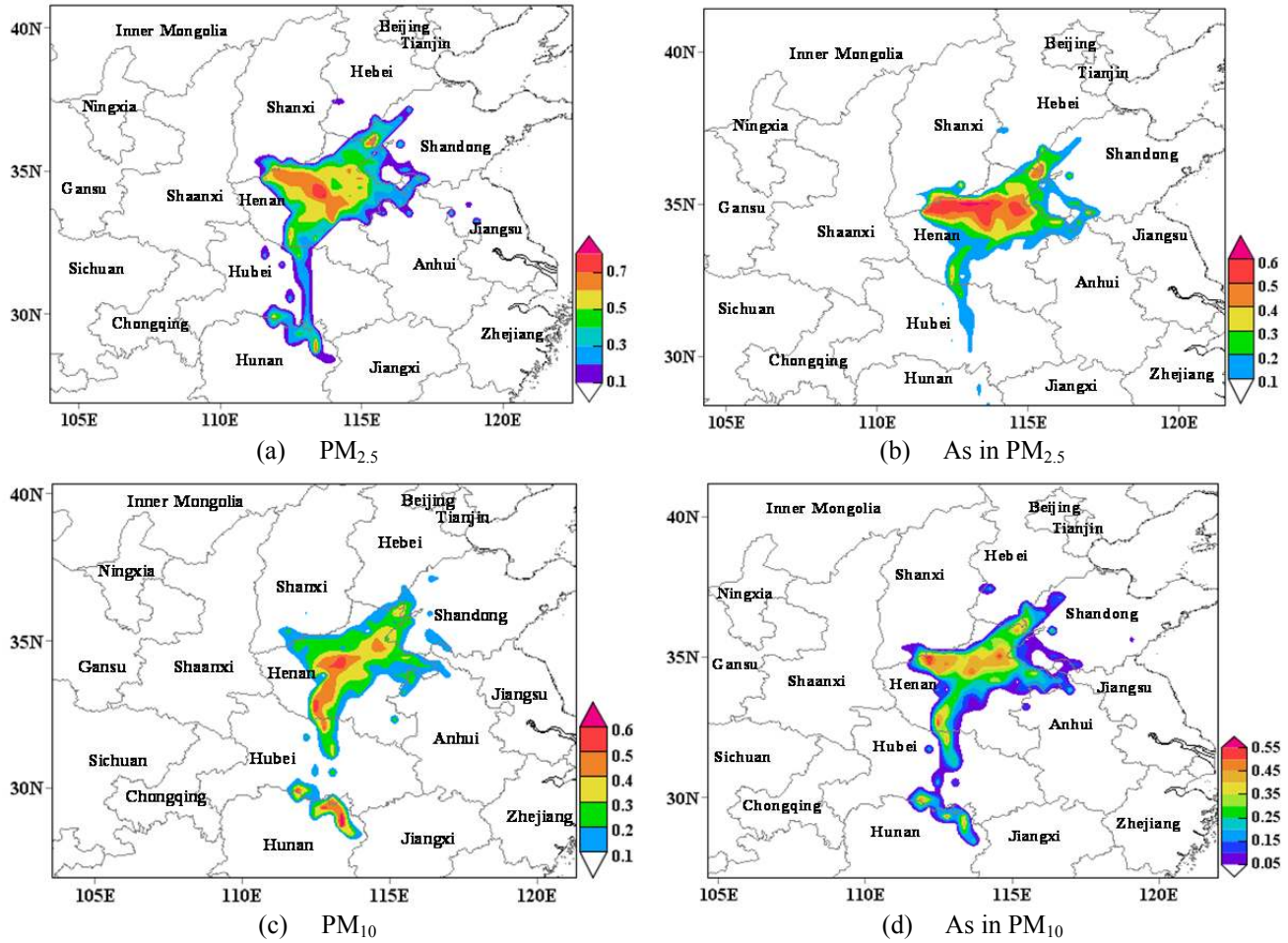

(a) $PM_{2.5}$ (b) As in $PM_{2.5}$

(c) PM_{10} (d) As in PM_{10}

Fig. 8. Spatial distributions of WPSCF values of $PM_{2.5}$, PM_{10}, and As in Zhengzhou in 2016.

CONCLUSION

$PM_{2.5}$ and PM_{10} filters were collected at five sites in Zhengzhou, and the concentrations, source apportionment, health risks, and source regions of the toxic elements were analyzed. The results indicated severe $PM_{2.5}$ and PM_{10} pollution, with annual average concentrations that were considerably higher than the Chinese NAAQS. The rural site (ZM) exhibited only slight pollution, but the traffic site (HKG) and the urban site with high traffic (SSQ) showed relatively high $PM_{2.5}$ levels, and the highest PM_{10} level was also observed at HKG. The highest and lowest mean levels were observed in winter and summer, respectively, for both $PM_{2.5}$ and PM_{10}.

Overall, high levels of PM-bound crustal elements and plentiful Cl indicated that dust and combustion sources played major roles. Furthermore, the PM_{10}-bound As greatly exceeded the Chinese NAAQS, posing a high potential risk. Generally, the total elemental levels were relatively low at ZM and high at GY, with high individual concentrations of Cl, Zn, Pb, and Cu, in particular, at the latter site. High levels of crustal elements were observed at SSQ and HKG, suggesting a significant influence from dust. High levels of crustal elements, which were more abundant in the PM_{10}, were observed in spring, whereas combustion-source elements, which were more abundant in the $PM_{2.5}$, displayed elevated levels in winter. The elemental concentrations were low in summer. In general, the CD values for the $PM_{2.5}$ were slightly higher than those for the PM_{10}. These results are not only related to discrepant spatial distributions of emission sources at the five sites but also attributable to different meteorological conditions across the four seasons.

The Na, Sb, Pb, Zn, Cu, and As were emitted from anthropogenic sources, whereas the Si, Mg, and Ti were crustal in origin. Pearson's CA, cluster analysis, and PCA indicated that vehicles, industry, coal combustion, oil fuel, dust, and biomass burning were probably the main sources of PM-bound elements in Zhengzhou. The ZM site was characterized by low traffic and high contributions from biomass burning and dust emission, whereas the HKG site demonstrated high pollution from traffic sources, and the SSQ site was also highly affected by pollution from vehicles. Whereas elements in the $PM_{2.5}$ largely originated in combustion sources, those in the PM_{10}, by comparison, received greater contributions from dust sources.

The PM-bound As and Ni posed both intolerable carcinogenic risks and, in addition to Pb, significant non-CRs. In general, children, as shown by higher CR and HQ values, were more sensitive than adults to these risks. The daily intake pathway exhibited the highest CR and HI values. Obvious differences in the CR and HI values were detected between the various sites; hence, data from multiple sites in a study area are necessary for accurate health risk assessment, especially for a large region. Analysis of the source regions identified Jiyuan, Jiaozuo, Xuchang, and Zhoukou; Pingdingshan and Nanyang; and Jiyuan, Jiaozuo, Xinxiang, Anyang, and Kaifeng as the main potential source areas of $PM_{2.5}$, PM_{10}, and As, respectively. Furthermore, fine particles with higher WPSCF values were more easily transmitted than coarse ones.

ACKNOWLEDGEMENTS

The study was supported by the financial support from the National Natural Science Foundation of China (51808510, 51778587), National Key Research and Development Program of China (2017YFC0212400), Natural Science Foundation of Henan Province of China (162300410255), Foundation for University Young Key Teacher by Henan Province (2017GGJS005), Outstanding Young Talent Research Fund of Zhengzhou University (1421322059) and Science and Technology Planning Project of Transportation in Henan Province (2016Y2-2, 2018J3).

SUPPLEMENTARY MATERIAL

Supplementary data associated with this article can be found in the online version at http://www.aaqr.org.

REFERENCES

AEA (2011). UK emissions of air pollutants 1970 to 2009. UK Emissions Inventory Team, Department for Environment, Food and Rural Affairs. http://uk-air.defra.gov.uk/reports/cat07/1401131501_NAEI_Annual_Report_2009.pdf.

Amato, F., Alastuey, A., Karanasiou, A., Lucarelli, F., Nava, S., Calzolai, G., Severi, M., Becagli, S., Gianelle, V.L., Colombi, C., Alves, C., Custódio, D., Nunes, T., Cerqueira, M., Pio, C., Eleftheriadis, K., Diapouli, E., Reche, C., Minguillón, M.C., Manousakas, M.I., Maggos, T., Vratolis, S., Harrison, R.M. and Querol, X. (2016). AIRUSE-LIFE+: A harmonized PM speciation and source apportionment in five southern European cities. *Atmos. Chem. Phys.* 16: 3289–3309.

Argyropoulos, G., Grigoratos, T., Voutsinas, M. and Samara, C. (2013). Concentrations and source apportionment of PM_{10} and associated elemental and ionic species in a lignite-burning power generation area of southern Greece. *Environ. Sci. Pollut. Res. Int.* 20: 7214–7230.

Ashbaugh, L.L., Malm, W.C. and Sadeh, W.Z. (1985). A residence time probability analysis of sulfur concentrations at Grand Canyon National Park. *Atmos. Environ.* 19: 1263–1270.

Bell, M.L. (2012). *Assessment of the health impacts of particulate matter characteristics*. Research Report 161. Health Effects Institute. Boston, MA, USA.

Bhangare, R.C., Ajmal, P.Y., Sahu, S.K., Pandit, G.G. and Puranik, V.D. (2011). Distribution of trace elements in coal and combustion residues from five thermal power plants in India. *Int. J. Coal Geol.* 86: 349–356.

Bozlaker, A., Spada, N.J., Fraser, M.P. and Chellam, S. (2013). Elemental characterization of $PM_{2.5}$ and PM_{10} emitted from light duty vehicles in the Washburn Tunnel of Houston, Texas: Release of rhodium, palladium, and platinum. *Environ. Sci. Technol.* 48: 54–62.

Bozlaker, A., Spada, N.J., Fraser, M.P. and Chellam, S. (2014). Elemental characterization of $PM_{2.5}$ and PM_{10} emitted from light duty vehicles in the Washburn Tunnel of Houston, Texas: Release of rhodium, palladium, and platinum. *Environ. Sci. Technol.* 48: 54–62.

Brunekreef, B. and Forsberg, B. (2005). Epidemiological evidence of effects of coarse airborne particles on health. *Eur. Respir. J.* 26: 309–318.

Bureau of Statistics of Henan Province (2017). Henan statistical yearbook 2017, China Statistics Press, Beijing (in Chinese). http://www.ha.stats.gov.cn/hntj/lib/tjnj/2017/indexch.htm.

Bureau of Statistics of Pingdingshan (2017). Statistical bulletins on national economic and social development of Pingdingshan in 2016 (in Chinese). http://pds.gov.cn/contents/4741/51885.html.

Bureau of Statistics of Zhengzhou (2017). Statistical Bulletins on national economic and social development of Zhengzhou in 2016 (in Chinese). http://tjj.zhengzhou.gov.cn/tjgb/418270.jhtml

Bytnerowicz, A., Omasa, K. and Paolletti, E. (2007). Integrated effects of air pollution and climate change on forest: A northern hemisphere perspective. *Environ. Pollut.* 147: 438–445.

Chao, C.Y. and Wong, K.K. (2002). Residential indoor PM_{10} and $PM_{2.5}$ in Hong Kong and the elemental composition. *Atmos. Environ.* 36: 265–277.

Charlesworth, S., De Miguel, E. and Ordonez, A. (2011). A review of the distribution of particulate trace elements in urban terrestrial environments and its application to considerations of risk. *Environ. Geochem. Health* 33: 103–123.

Contini, D., Belosi, F., Gambaro, A., Cesari, D., Stortini, A.M. and Bove, M.C. (2012). Comparison of PM_{10} concentrations and metal content in three different sites of the Venice lagoon: An analysis of possible aerosol sources. *J. Environ. Sci.* 24: 1954–1965.

Diaz, R.V. and Dominguez, E.R. (2009). Health risk by inhalation of $PM_{2.5}$ in the metropolitan zone of the City of Mexico. *Ecotoxicol. Environ. Saf.* 72: 866–871.

Dunea, D., Iordache, S, Liu, H.Y., Bøhler, T. and Pohoata, A. (2016). Quantifying the impact of $PM_{2.5}$ and associated heavy metals on respiratory health of children near metallurgical facilities. *Environ. Sci. Pollut. Res. Int.* 23: 15395–15406.

Eldred, R.A., Cahill, T.A. and Flocchini, R.G. (1997). Composition of $PM_{2.5}$ and PM_{10} aerosols in the IMPROVE network. *J. Air Waste Manage. Assoc.* 47: 194–203.

Fang, G.C., Huang, Y.L. and Huang, J.H. (2010). Study of atmospheric metallic elements pollution in Asia during 2000–2007. *J. Hazard. Mater.* 180: 115–121.

Fang, G.C., Wu, Y.S., Wen, C.C., Huang, S.H. and Rau, J.Y. (2006). Ambient air particulate concentrations and metallic elements principal component analysis at Taichung Harbor (TH) and WuChi Traffic (WT) near Taiwan Strait during 2004–2005. *J. Hazard. Mater.* 137: 314–323.

Feng, Y.C., Xue, Y.H., Chen, X.H., Wu, J.H., Zhu, T., Bai, Z.P., Fu, S.T. and Gu, C.J. (2007). Source apportionment of ambient total suspended particulates and coarse particulate matter in urban areas of Jiaozuo, China. *J. Air Waste Manage. Assoc.* 57: 561–575.

Guo, Y.M., Tong, S.L., Zhang, Y.S., Barnett, A.G., Jia, Y.P. and Pan, X.C. (2010). The relationship between particulate air pollution and emergency hospital visits for hypertension in Beijing, China. *Sci. Total Environ.* 408: 4446–4450.

Hadley, O.L. (2017). Background $PM_{2.5}$ source apportionment in the remote Northwestern United States. *Atmos. Environ.* 167: 298–308.

Han, B., Kong, S.F., Bai, Z.P., Du, G., Bi, T., Li, X., Shi, G.L. and Hu, Y.D. (2010). Characterization of elemental species in $PM_{2.5}$ samples collected in four cities of northeast China. *Water Air Soil Pollut.* 209: 15–28.

Hopke, P.K., Barrie, L.A., Li, S.M., Cheng, M.D., Li, C. and Xie, Y. (1995). Possible sources and preferred pathways for biogenic and non-sea-salt sulfur for the high Arctic. *J. Geophys. Res.* 100: 16595–16603.

Hsu, C.Y., Chiang, H.C., Lin, S.L., Chen, M.J., Lin, T.Y. and Chen, Y.C. (2016). Elemental characterization and source apportionment of PM_{10} and $PM_{2.5}$ in the western coastal area of central Taiwan. *Sci. Total Environ.* 541, 1139–1150.

Hsu, Y.K., Holsen, T.M. and Hopke, P.K. (2003). Comparison of hybrid receptor models to locate PCB sources in Chicago. *Atmos. Environ.* 37: 545–562.

Hu, X., Zhang, Y., Ding, Z.H., Wang, T.J., Lian, H.Z., Sun, Y.Y. and Wu, J.C. (2012). Bioaccessibility and health risk of arsenic and heavy metals (Cd, Co, Cr, Cu, Ni, Pb, Zn and Mn) in TSP and $PM_{2.5}$ in Nanjing, China. *Atmos. Environ.* 57: 146–152.

Jeong, U., Kim, J., Lee, H., Jung, J., Kim, Y., Song, C. and Koo, J. (2011). Estimation of the contributions of long range transported aerosol in East Asia to carbonaceous aerosol and PM concentrations in Seoul, Korea using highly time resolved measurements: A PSCF model approach. *J. Environ. Monit.* 13: 1905–1918.

Ji, D., Li, L., Wang, Y., Zhang, J., Cheng, M., Sun, Y., Liu, Z., Wang, L., Tang, G., Hu, B., Chao, N., Wen, T. and Miao, H. (2014). The heaviest particulate air-pollution episodes occurred in northern China in January, 2013: Insights gained from observation. *Atmos. Environ.* 92: 546–556.

Jiang, N., Guo, Y., Wang, Q., Kang, P.R., Zhang, R.Q. and Tang, X.Y. (2017). Chemical composition characteristics of $PM_{2.5}$ in three cities in Henan, central China. *Aerosol Air Qual. Res.* 17: 2367–2380.

Jiang, N., Dong, Z., Xu, Y.Q., Yu, F., Yin, S.S., Zhang, R.Q. and Tang, X.Y. (2018a). Characterization of PM_{10} and $PM_{2.5}$ source profiles of fugitive dust in Zhengzhou, China. *Aerosol Air Qual. Res.* 18: 314–329.

Jiang, N., Duan, S.G., Yu, X., Zhang, R.Q. and Wang, K. (2018b). Comparative major components and health risks of toxic elements and polycyclic aromatic hydrocarbons of $PM_{2.5}$ in winter and summer in Zhengzhou: Based on three-year data. *Atmos. Res.* 213: 173–184.

Jiang, N., Li, Q., Su, F.C., Wang, Q., Yu, X., Kang, P.R.,

Zhang, R.Q. and Tang, X.Y. (2018c). Chemical characteristics and source apportionment of $PM_{2.5}$, between heavily polluted days and other days in Zhengzhou, China. *J. Environ. Sci.* 66: 188–198.

Jiang, N., Wang, K., Yu, X., Su, F.C., Yin, S.S., Li, Q. and Zhang, R.Q. (2018d). Chemical characteristics and source apportionment by two receptor models of size-segregated aerosols in an emerging megacity in China. *Aerosol Air Qual. Res.* 18: 1375–1390.

Jiang, N., Yin, S.S., Guo, Y., Li, J.Y., Kang, P.R., Zhang, R.Q. and Tang, X.Y. (2018e). Characteristics of mass concentration, chemical composition, source apportionment of $PM_{2.5}$ and PM_{10} and health risk assessment in the emerging megacity in China. *Atmos. Pollut. Res.* 9: 309–321.

Jiang, N., Li, L.P., Wang, S.S., Li, Q., Dong, Z., Duan, S.G., Zhang, R.Q. and Li, S.L. (2019). Variation tendency of pollution characterization, sources, and health risks of $PM_{2.5}$-bound polycyclic aromatic hydrocarbons in an emerging megacity in China: Based on three-year data. *Atmos. Res.* 217: 81–92.

Kang, Y., Liu, M., Song, Y., Huang, X., Yao, H., Cai, X., Zhang, H., Kang L., Liu X., Yan, X., He, H., Zhang Q., Shao, M. and Zhu, T. (2016). High-resolution ammonia emissions inventories in China from 1980 to 2012. *Atmos. Chem. Phys.* 16: 2043–2058.

Li, Q., Jiang, N., Yu, X., Dong, Z., Duan, S., Zhang, L. and Zhang, R. (2019). Sources and spatial distribution of $PM_{2.5}$-bound polycyclic aromatic hydrocarbons in Zhengzhou in 2016. *Atmos. Res.* 216: 65–75.

Li, Y., Zhang, Z., Liu, H., Zhou, H., Fan, Z., Lin, M., Wu, D. and Xia, B. (2016). Characteristics, sources and health risk assessment of toxic heavy metals in $PM_{2.5}$ at a megacity of southwest China. *Environ. Geochem. Health* 38: 353–362.

Li, Y., Miao, C., Ding, S., Wang, S., Ni, D. and Hu, H. (2017). Monitoring and source apportionment of trace elements in $PM_{2.5}$: Implications for local air quality management. *J. Environ. Manage.* 196: 16–25.

Liao, T., Wang, S., Ai, J., Gui, K., Duan, B., Zhao, Q., Zhang, X., Jiang, W. and Sun, Y. (2017). Heavy pollution episodes, transport pathways and potential sources of $PM_{2.5}$ during the winter of 2013 in Chengdu (China). *Sci. Total Environ.* 584–585: 1056–1065.

Mancilla, Y. and Mendoza, A. (2012). A tunnel study to characterize $PM_{2.5}$ emissions from gasoline-powered vehicles in Monterrey, Mexico. *Atmos. Environ.* 59: 449–460.

Mason, S. (1966). *Principles of geochemistry*. Wiley, New York, USA, pp. 45–46.

Ministry of Environmental Protection of the People's Republic of China (2017). Report on the State of the Environment in China in 2016. http://english.mep.gov.cn/Resources/Reports/soe/ReportSOE/201709/P020170929573904364594.pdf.

Moosmüller, H., Chakrabarty, R.K. and Arnott, W.P. (2009). Aerosol light absorption and its measurement: A review. *J. Quant. Spectrosc. Radiat. Transfer* 110: 844–878.

National Bureau of Statistical of China (2015). China statistical yearbook 2015. China Statistics Press, Beijing. http://www.stats.gov.cn/tjsj/ndsj/2016/indexch.htm.

National Health and Family Planning Commission of the People's Republic of China (2013). China health statistical yearbook in 2010. http://www.nhfpc.gov.cn/htmlfiles/zwgkzt/ptjnj/year2013/index2013.html.

Nolting, R.F., Ramkema, A. and Everaarts, J.M. (1999). The geochemistry of Cu, Cd, Zn, Ni and Pb in sediment cores from the continental slope of the Banc d'Arguin (Mauritania). *Cont. Shelf Res*. 19: 665–691.

Ny, M.T. and Lee, B.K. (2011). Size distribution of airborne particulate matter and associated metallic elements in an urban area of an industrial city in Korea. *Aerosol Air Qual. Res.* 11: 643–653.

Okuda, T., Katsuno, M., Naoi, D., Nakao, S., Tanaka, S., He, K.B., Ma, Y.L., Lei, Y. and Jia, Y.T. (2008). Trends in hazardous trace metal concentrations in aerosols collected in Beijing, China from 2001 to 2006. *Chemosphere* 72: 917–924.

Pan, Y., Wang, Y., Sun, Y., Tian, S. and Cheng, M. (2013). Size-resolved aerosol trace elements at a rural mountainous site in Northern China: Importance of regional transport. *Sci. Total Environ.* 461–462: 761–771.

Peng, G.L., Wang, X.M., Wu, Z.Y., Wang, Z.M., Yang, L.L., Zhong, L.J. and Chen, D.H. (2011). Characteristics of particulate matter pollution in the Pearl River Delta region, China: An observational-based analysis of two monitoring sites. *J. Environ. Monitor.* 13: 1927–1934.

Polissar, A.V., Hopke, P.K., Paatero, P., Kaufmann, Y.J., Hall, D.K., Bodhaine, B.A., Dutton, E.G. and Harris, J.M. (1999). The aerosol at Barrow, Alaska: Long-term trends and source locations. *Atmos. Environ.* 33: 2441–2458.

Pope, C.A. and Dockery, D.W. (2006). Health effects of fine particulate air pollution: Lines that connect. *J. Air Waste Manage. Assoc.* 56: 709–742.

Querol, X., Zhuang, X., Alastuey, A., Viana, M., Lv, W., Wang, Y., Lopez, A., Zhu, Z., Wei, H. and Xu, S. (2006). Speciation and sources of atmospheric aerosols in a highly industrialized merging mega-city in Central China. *J. Environ. Monit.* 8: 1049–1059.

Ren, L.H., Zhang, R.J., Bai, Z.P., Chen, J.H., Liu, H.J., Zhang, M.G., Yang, X.Y. and Zhang, L.M. (2012). Aircraft measurements of ionic and elemental components in $PM_{2.5}$ over Eastern Coastal area of China. *Aerosol Air Qual. Res.* 12: 1237–1246.

Robin, T., Guidi, L., Dufour, A. and Migon, C. (2013). Statistical distributions of trace metal concentrations in the northwestern Mediterranean atmospheric aerosol. *Environ. Monit. Assess.* 185: 9177–9189.

Silva, P.J., Liu, D.Y., Noble, C.A. and Prather, K.A. (1999). Size and chemical characterization of individual particles resulting from biomass burning of local southern California species. *Environ. Sci. Technol.* 33: 3068–3076.

Sun, Y., Hu, X., Wu, J., Lian, H. and Chen, Y. (2014). Fractionation and health risks of atmospheric particle-bound As and heavy metals in summer and winter. *Sci. Total Environ.* 493: 487–494.

Taiwo, A.M., Harrison, R.M. and Shi, Z. (2014). A review of receptor modeling of industrially emitted particulate matter. *Atmos. Environ.* 97: 109–120.

Tao, M., Chen, L., Wang, Z., Wang, J., Tao, J. and Wang, X. (2016). Did the widespread haze pollution over China increase during the last decade? A satellite view from space. *Environ. Res. Lett.* 11: 054019.

Tsai, J.H., Lin, K.H., Chen, C.Y., Ding, J.Y., Choa, C.G. and Chiang, H.L. (2007). Chemical constituents in particulate emissions from integrated iron and steel facility. *J. Hazard. Mater.* 147: 111–119.

U.S. EPA (1989). Risk assessment guidance for superfund. In: Part A: Human Health Evaluation Manual. https://www.epa.gov/risk/risk-assessment-guidance-superfund-rags-part

U.S. EPA (1999). Determination of metals in ambient particulate matter using X-ray Fluorescence (XRF) spectroscopy. https://www3.epa.gov/ttn/amtic/files/ambient/inorganic/mthd-3-3.pdf.

U.S. EPA (2004). Risk assessment guidance for superfund. In: Part E, Supplemental guidance for dermal risk assessment. https://www.epa.gov/risk/risk-assessment-guidance-superfund-rags-part.

U.S. EPA (2009). Risk assessment guidance for superfund. In: Part F, Supplemental Guidance for Inhalation Risk Assessment. https://www.epa.gov/risk/risk-assessment-guidance-superfund-rags-part.

U.S. EPA (2017). The Screening Level (RSL) tables (Last updated June 2017). https://www.epa.gov/risk/regional-screening-levels-rsls-generic-tables-june-2017.

Viana, M., Querol, X., Alastuey, A., Gil, J.I. and Menéndez, M. (2006). Identification of PM sources by principal component analysis (PCA) coupled with wind direction data. *Chemosphere* 65: 2411–2418.

Viana, M., Kuhlbusch, T.A.J., Querol, X., Alastuey, A., Harrison, R.M., Hopke, P.K., Winiwarter, W., Vallius, M., Szidat, S., Prévôt, A.S.H., Hueglin, C., Bloemen, H., Wåhlin, P., Vecchi, R., Miranda, A.I., Kasper-Giebl, A., Maenhaut, W. and Hitzenberger, R. (2008). Source apportionment of particulate matter in Europe: A review of methods and results. *J. Aerosol Sci.* 39: 827–849.

Wang, J., Hu, Z.M., Chen, Y.Y., Chen, Z.L. and Xu, S.Y. (2013). Contamination characteristics and possible sources of PM_{10} and $PM_{2.5}$ in different functional areas of Shanghai, China. *Atmos. Environ.* 68: 221–229.

Wang, Q., Jiang, N., Yin, S.S., Li, X., Yu, F., Guo, Y. and Zhang R.Q. (2017). Carbonaceous species in $PM_{2.5}$, and PM_{10}, in urban area of Zhengzhou in China: Seasonal variations and source apportionment. *Atmos. Res.* 191: 1–11.

Wang, S.B., Yan, Q.S., Yu, F., Wang, Q., Yang, L.M., Zhang, R.Q. and Yin, S.S. (2018). Distribution and source of chemical elements in size-resolved particles in Zhengzhou, China: Effects of regional transport. *Aerosol Air Qual. Res.* 18: 371–385.

Wang, Y., Hu, M., Wang, Y., Qin, Y., Chen, H., Zeng, L., Lei, J., Huang, X., He, L., Zhang, R. and Wu, Z. (2016). Characterization and influence factors of $PM_{2.5}$ emitted from crop straw burning. *Acta Chim. Sinica* 74: 356–362.

Wang, Z.S., Duan, X.L., Liu, P., Nie, J., Huang, N. and Zhang, J.L. (2009). Human exposure factors of Chinese people in environmental health risk assessment. *Res. Environ. Sci.* 22: 1164–1170 (in Chinese).

Wei, F. (1990). *The element background values of Chinese soil*. China Environmental Science Press, Beijing, China.

Winner, D.A. and Cass, G.R. (2001). Modeling the long-term frequency distribution of regional ozone concentrations using synthetic meteorology. *Environ. Sci. Technol.* 35: 3718–3726.

Wongphatarakul, V., Friedlander, S.K. and Pinto, J.P. (1998). A comparative study of $PM_{2.5}$ ambient aerosol chemical databases. *J. Aerosol Sci.* 29: S115–S116.

Wu, Y.S., Fang, G.C., Lee, W.J., Lee, J.F., Chang, C.C. and Lee, C.Z. (2007). A review of atmospheric fine particulate matter and its associated trace metal pollutants in Asian countries during the period 1995–2005. *J. Hazard. Mater.* 143: 511–515.

Yang, Y.R., Liu, X.G., Qu, Y., An, J.L., Jiang, R., Zhang, Y.H., Sun, Y.L., Wu, Z.J., Zhang, F., Xu, W.Q. and Ma, Q.X. (2015). Characteristics and formation mechanism of continuous hazes in China: a case study during the autumn of 2014 in the North China Plain. *Atmos. Chem. Phys.* 15: 8165–8178.

Yao, Q., Li, S.Q., Xu, H.W., Zhuo, J.K. and Song, Q. (2009). Studies on formation and control of combustion particulate matter in China: A review. *Energy* 34: 1296–1309.

Yu, F., Yan, Q., Jiang, N., Su, F., Zhang, L., Yin, S., Li, Y. and Zhang R. (2016). Tracking pollutant characteristics during haze events at background site Zhongmu, Henan province, China. *Atmos. Pollut. Res.* 8: 64–73.

Zhang, R., Jing, J., Tao, J., Hsu, S. C., Wang G., Cao J., Lee, C.S.L., Zhu, L., Chen, Z., Zhao, Y. and Shen, Z. (2013). Chemical characterization and source apportionment of $PM_{2.5}$ in Beijing: Seasonal perspective. *Atmos. Chem. Phys.* 13: 7053–7074.

Zhang, X.Y., Gong, S.L., Shen, Z.X., Mei, F.M., Xi, X.X., Liu, L.C., Zhou, Z.J., Wang, D., Wang, Y.Q. and Cheng, Y. (2003). Characterization of soil dust aerosol in China and its transport and distribution during 2001 ACE-Asia: 1. Network observations. *J. Geophys. Res.* 108: 1–13.

Zhang, Y., Wang, X., Chen, H., Yang, X., Chen, J. and Allen, J.O. (2009). Source apportionment of lead-containing aerosol particles in Shanghai using single particle mass spectrometry. *Chemosphere* 74: 501–507.

Zhengzhou Municipal Environmental Protection Bureau (2016). The closed and production suspended progress of environmental illegal construction projects in Zhengzhou (in Chinese). http://www.zzepb.gov.cn/Article/Content/?id=35269.

Received for review, July 25, 2018
Revised, November 5, 2018
Accepted, November 21, 2018